Patterns of hybrid seed inviability in perennials of the *Mimulus guttatus* sp. complex reveal a potential role of parental conflict in reproductive isolation

Jenn M. Coughlan[1,2], Maya Wilson Brown[1], John H. Willis[1]

1. *Biological Sciences, Duke University 25 Science Drive, Durham NC*
2. *Biology Department, University of North Carolina, Chapel Hill*

Lead Contact: *Jenn M. Coughlan*

Key Words: *Speciation, Endosperm, BDMIs, arms race, cryptic species*

Running headline: *Parental conflict & hybrid seed inviability*

Summary

Genomic conflicts may play a central role in the evolution of reproductive barriers. Theory predicts that early-onset hybrid inviability may stem from conflict between parents for resource allocation to offspring. Here we describe *M. decorus;* a group of cryptic species within the *M. guttatus* species complex that are largely reproductively isolated by hybrid seed inviability (HSI). HSI between *M. guttatus* and *M. decorus* is common and strong, but populations of *M. decorus* vary in the magnitude and directionality of HSI with *M. guttatus*. Patterns of HSI between *M. guttatus* and *M. decorus,* as well as within *M. decorus* conform to the predictions of parental conflict: (1) reciprocal F1s exhibit size differences and parent-of-origin specific endosperm defects, (2) the extent of asymmetry between reciprocal F1 seed size is correlated with asymmetry in HSI, and (3) inferred differences in the extent of conflict predict the extent of HSI between populations. We also find that HSI is rapidly evolving, as populations that exhibit the most HSI are each others' closest relative. Lastly, while all populations are largely outcrossing, we find that the differences in the inferred strength of conflict scale positively with π, suggesting that demographic or life history factors other than mating system may also influence the rate of parental conflict driven evolution. Overall, these patterns suggest the rapid evolution of parent-of-origin specific resource allocation alleles coincident with HSI within and between *M. guttatus* and *M. decorus.* Parental conflict may therefore be an important evolutionary driver of reproductive isolation.

Introduction

The origin and maintenance of species ultimately depends on the formation of reproductive barriers between populations. Research to date has highlighted the role of ecological and sexual selection in the formation of many pre-zygotic and extrinsic post-zygotic barriers (e.g. Bradshaw & Schemske 2003; Ramsey & Schemske 2003; Nosil *et al.* 2005; Arngard *et al.* 2014). However, relatively less is known about the evolutionary forces driving the formation of intrinsic barriers.

The formation of early-onset hybrid inviability is a common and powerful intrinsic reproductive barrier in nature (Tiffin *et al.* 2001; Lowry *et al.* 2008), especially in placental mammals (e.g. Vranna *et al.* 2000; Zechner *et al.* 2004; Brekke *et al.* 2014, 2016) and seed plants (e.g. Scott *et al.* 1998; Wolff *et al.* 2015; Rebernig *et al.* 2015; Oneal *et al.* 2016; Garner *et al.* 2016; Roth *et al.* 2017). One hypothesis to explain the evolution of early-onset hybrid inviability is that of parental conflict (Trivers 1974; Charnov 1979; Haig & Westoby 1989). Parental conflict can arise in non-monogamous systems because maternal and paternal optima for resource allocation to offspring differ (Trivers 1974; Charnov 1979; Haig & Westoby 1989). Since maternity is guaranteed, selection should favor equivalent resource allocation from mothers to children. However, in non-monogamous systems, selection should favor the evolution of paternally derived alleles that increase resource allocation to offspring (Trivers 1974; Charnov 1979; Haig & Westoby 1989). Therefore, a co-evolutionary arms race for resource-acquiring paternal

64 alleles and resource-repressive maternal alleles can evolve. Reproductive isolation can
65 manifest if populations have evolved at different rates and/or with different genetic
66 responses to conflict, resulting in a mismatch between maternal and paternal alleles in
67 hybrids. While there is some evidence for parental conflict dynamics within species (e.g.
68 Willi 2013; Raunsgard *et al.* 2018; Cailleau *et al.* 2018), the role of parental conflict in the
69 evolution of reproductive isolation requires further study.

70 Parental conflict poses an enticing hypothesis for the evolution of early-onset
71 hybrid inviability, because early-onset hybrid inviability is common in systems that
72 partition resources after fertilization (e.g. seed plants and placental mammals; Vranna
73 2007; Lafon-Placette & Köhler 2016) relative to systems that do not (e.g. birds and frogs;
74 Wilson *et al.* 1974; Prager & Wilson 1975; Fitzpatrick 2004). It is also consistent with the
75 observation that many examples of early-onset hybrid inviability are asymmetric (e.g.
76 Vranna *et al.* 2000; Rebernig *et al.* 2015), and arise from issues of excessive or limited
77 growth, consistent with the idea that these incompatibilities involve parent-of-origin
78 resource allocation alleles (i.e. alleles whose effects are mediated by whether they are
79 maternally or paternally inherited; Vranna *et al.* 2000; Rebernig *et al.* 2015; Oneal *et al.*
80 2016). Yet, hybrid inviability may also evolve as a byproduct of other selective pressures
81 (e.g. ecological differences), through neutral processes (e.g. gene duplication; Lynch &
82 Force 2000), or other sources of conflict (e.g. TE/repressor dynamics Martienssen 2010;
83 Castillo & Moyle 2012). As most studies of early-onset hybrid inviability are based on a
84 single population pair, (e.g. Vranna *et al.* 2000; Rebernig *et al.* 2015; Wolff *et al.* 2015;

85 Brekke *et al.* 2016), we lack a comparative framework for understanding whether
86 parental conflict can shape early-onset hybrid inviability, and what factors affect the
87 magnitude and direction of inviability.

88 In seed plants, parental conflict is thought to manifest in the endosperm- a
89 nutritive tissue that is essential for proper embryo development (Köhler *et al.* 2010). Like
90 the mammalian placenta, endosperm represents a direct nutritive connection between
91 developing offspring and mother. Unlike placenta, endosperm is a triploid tissue that is
92 comprised of 2:1 maternal:paternal genetic composition. In inter-ploidy crosses- where
93 hybrid seed inviability (HSI) has been best studied- departures from this 2:1 ratio often
94 result in irregular endosperm growth, and seed death, even if the embryo itself is viable
95 (Lin 1984; Scott *et al.* 1998; 'triploid block'- Comai 2005; Köhler *et al.* 2010). In *Arabidopsis*
96 inter-ploidy crosses, improper dosage of normally imprinted genes in the endosperm
97 cause endosperm irregularities and ultimately, inviability (Kradolfer *et al.* 2013; Wolff *et*
98 *al.* 2015). Because of the shared phenotypic defects in HSI between intra-diploid and
99 inter-ploidy crosses (e.g. Lafon-Placette *et al.* 2017), many researchers use 'effective
100 ploidy' or 'Endosperm Balance Number' (EBN) as a way to quantify the strength of
101 conflict of a given species relative to another, regardless of actual ploidy (Johnson *et al.*
102 1980). While EBNs can be used to describe differences in both inter-ploidy and intra-
103 diploid crosses, the underlying genetic mechanisms between these two types of crosses
104 may differ. While inter-ploidy HSI can be caused by differences in dosage of maternal
105 versus paternal alleles as a result of whole genome duplication, intra-diploid HSI must

106 be caused by either sequence change or duplication of specific genes. Whether parental
107 conflict is responsible for genic changes that contribute to HSI among diploids remains
108 relatively unexplored (but see Lafon-Placette *et al.* 2018).

109 The strength of reproductive isolation often varies between populations
110 (Sweigart *et al.* 2007; Bomblies *et al.* 2007; Case & Willis, 2008; Martin & Willis, 2010;
111 Sicard *et al.* 2015; Case *et al.* 2016; Barnard-Kubow & Galloway, 2017; Bracewell *et al.*
112 2017). Leveraging this natural variation can help researchers to test the potential
113 evolutionary drivers responsible for different reproductive barriers. If parental conflict
114 drives the evolution of HSI, we would predict that (1) reciprocal F1 seeds should show
115 differences in size, indicating parent-of-origin effects on growth. (2) If these parent-of-
116 origin effects on growth cause reproductive isolation, then the degree of asymmetry in
117 reciprocal F1 size should correlate with inviability. Lastly, (3) differences in the strength
118 of conflict between populations (e.g. differences in EBN between populations) should
119 predict the degree of reproductive isolation in subsequent crosses.

120 We use the *Mimulus guttatus* species complex as a system to study the evolution
121 of HSI. The *Mimulus guttatus* species complex is a diverse group of wildflowers that are
122 well known for adaptations to extreme ecological conditions (e.g. Lowry *et al.* 2009;
123 Wright *et al.* 2013; Ferris & Willis 2018; Selby & Willis 2018), mating system evolution
124 (Fishman *et al.* 2002; Martin & Willis 2007; Brandvain *et al.* 2014; Fishman *et al.* 2015), and
125 life history variation (Hall *et al.* 2006; Lowry *et al.* 2010; Friedman *et al.* 2015; Peterson *et*
126 *al.* 2016), and is a model system for ecology, evolution, and genetics (Wu *et al.* 2008;

127 Twyford *et al.* 2015). The group consists of both annual and perennial species, and while
128 many annual species have been well studied (e.g. Martin & Willis 2007; Sweigart *et al.*
129 2006; Peterson *et al.* 2013; Oneal *et al.* 2016; Ferris & Willis 2018; Toll & Willis 2019),
130 studies of perennials in this group have been largely limited to morphological anecdotes
131 (Grant 1924, Nesom 2012). Thus we lack a basic understanding of the diversity of species
132 in one of the most well studied, non-crop plant systems (Lowry *et al. in press*).
133 Here we combine a common garden experiment, population genomics, and
134 quantification of reproductive isolation to reveal the presence of a cryptic species
135 complex- *M. decorus*- nested within the *M. guttatus* species complex. Using both crossing
136 and developmental surveys, we find that reproductive isolation between these cryptic
137 species is largely conferred via HSI. We leverage diversity in the extent and direction of
138 HSI in this group to assess the role of parental conflict in the evolution of HSI.

139

140 ## Results

141 ***M. decorus* is a phenotypically cryptic, but genetically distinct group of species**

142 In order to assess the phenotypic and genetic divergence between perennial
143 members of the *M. guttatus* species complex we combined previously published
144 genomic datasets with new re-sequencing data and performed a common garden
145 experiment. While several perennial morphological variants have been described based
146 on subtle phenotypic differences (Grant 1924, Nesom 2012), it remains unknown
147 whether these morphological variants comprise reproductively isolated species or are

148 simply localized morphological oddities. We find that one such morphological variant-
149 *M. decorus*- is genetically unique from other perennial variants in the *M. guttatus* species
150 complex, despite minimal phenotypic divergence (Fig. 1; also see Coughlan & Willis
151 2018). In contrast, populations of annual, inland perennial, and coastal perennial *M.*
152 *guttatus* show minimal genetic separation despite substantial phenotypic differentiation
153 among life histories types (Fig. 1, Fig. S1, S2 & S3; also see Twyford & Friedman 2016).
154 *Mimulus decorus* can further be categorized into three genetic clusters: a northern diploid
155 that occur in the central Cascade Mountains of Oregon, a southern diploid group from
156 the southern Cascades, and several tetraploids that occur primarily in the northern end
157 of the range (Fig. 1, Fig. S1 & S2).

158 Neighbor-joining trees also place *M. decorus* as a monophyletic group that is is
159 sister to *M. guttatus,* with the more divergent *M. tilingii* as an outgroup (Fig.1; Fig. S3).
160 Divergence between *M. decorus* and *M. guttatus* is similar to that of the recently diverged
161 *M. guttatus* and *M. nasutus* (genome-wide d_{xy} using 4-fold degenerate sites between *M.*
162 *guttatus* and *M. decorus* is 5.7% and 5.8% for the northern and southern clades of *M.*
163 *decorus,* respectively, and 5.8% between *M. guttatus* and *M. nasutus*; Table S7; Brandvain
164 *et al.* 2014). In contrast, divergence between more distantly related species *M. guttatus*
165 and *M. tilingii* is 6.5% (Table S7; Garner *et al.* 2016) Using the same approach as
166 Brandvain *et al.* 2014, we estimate the split between *M. guttatus* and *M. decorus* to be
167 approximately 230 kya (i.e. $t = \pi_{guttxdec} - \pi_{dec}/2\mu$, where μ is estimated to be 1.5×10^{-8}.
168 Therefore, $t = 0.007/2\mu = \sim 233$ ky). Northern and southern clades of *M. decorus* may thus

represent a relatively recent split from *M. guttatus*, and/or have experienced substantial introgression with *M. guttatus* post secondary contact. In order to determine if this population genetic structuring is a consequence of reproductive isolation between these taxa, we next assessed crossing barriers between *M. guttatus* and *M. decorus* by completing a range-wide crossing survey.

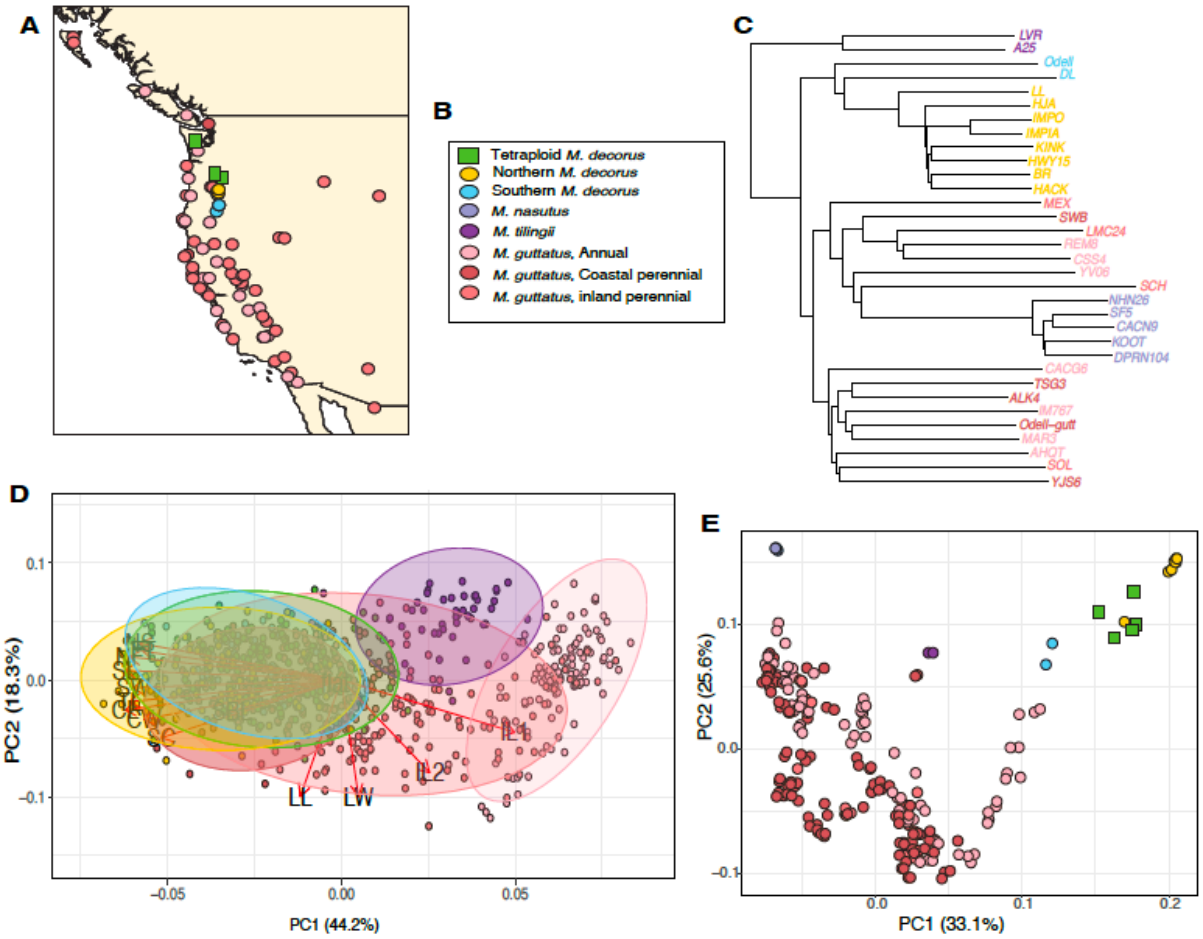

Figure 1: Phenotypic and genetic description of focal members of the *M. guttatus* species complex. (A) Geographic sampling of genetic samples from *M. guttatus* and *M. decorus*. Inland versus coastal perennials were not distinguished in the previous study and are thus both indicated by darker pink points in this panel. (B) Legend of the colors used to denote each species (C) NJ tree constructed using 4-fold degenerate sites and rooted using *M. dentilobus*. (D) PCA of 15 morphological characteristics for perennials within the *M. guttatus* species complex, as well as

perennial *M. tilingii* and annual *M. guttatus*. Trait codes as follows: FT- days to first flower, FN- node of first flower, ST-stem thickness, CW- corolla width, TL- tube length, CL- corolla length, LL- leaf length, LW- leaf width, IL1- first internode length, IL2- second internode length, NS- number of stolons, SL- stolon length, SW- stolon width, SBL- side branch length, NSB- number of side branches. (E) PCA of re-sequencing data for focal members of the *M. guttatus* species complex. In both PCAs the percent of total variance explained by that PC is indicated in parentheses.

Hybrid seed inviability is a significant, but variable reproductive barrier between *M. decorus* and *M. guttatus*

There is significant HSI between *M. guttatus* and each genetic clade of *M. decorus* (Fig. 2; RI is 0.53, 0.39, and 0.38 for *M. guttatus* and northern, southern, and tetraploid *M. decorus,* respectively; see Table S2 for RI measures for each population). However, we find no evidence for a reduction in seed set in interspecific crosses relative to intraspecific crosses (Fig. S8). Thus, while there is limited reproductive isolation conferred by pollen pistil interactions, HSI imposes a substantial reproductive barrier.

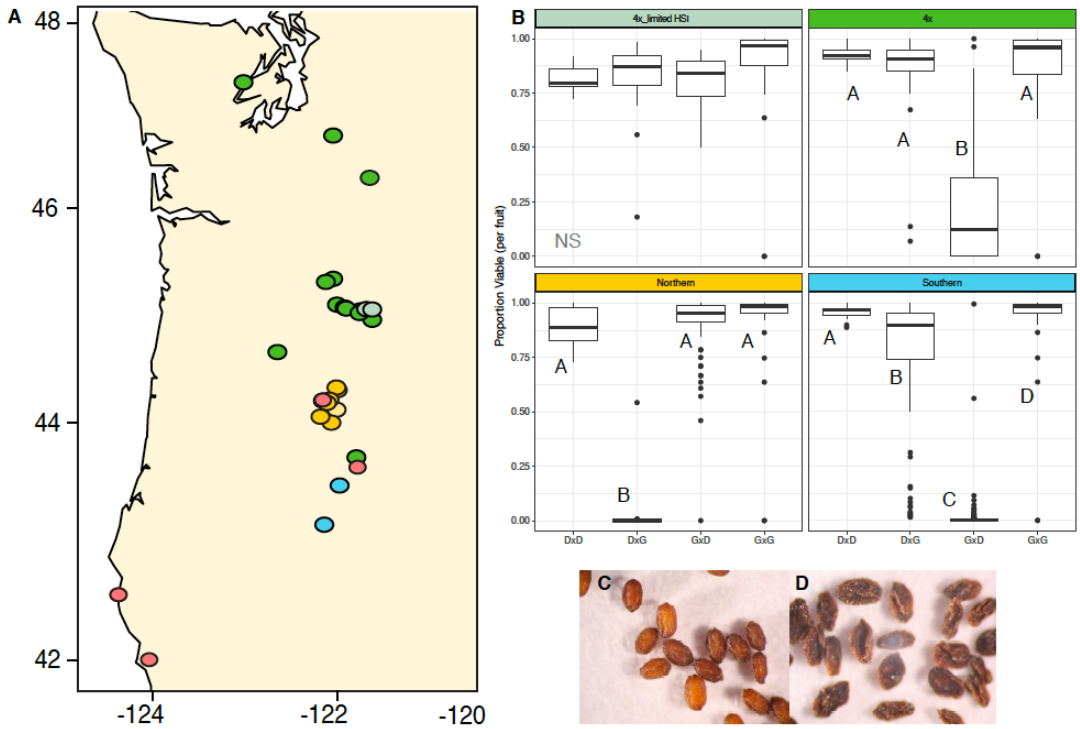

Figure 2: Geographic distribution of hybrid seed inviability between *M. decorus* and *M. guttatus*. (A) Sampling locales of 19 populations of *M. decorus* that were crossed to four *M. guttatus* populations reciprocally. Points are colored as in Fig.1, but points which are lighter in hue are populations that exhibit limited reproductive isolation with *M. guttatus*. (B) Crossing patterns for four populations of *M. decorus*, representing the four main crossing phenotypes observed (from top left to bottom right): 2 populations of tetraploid *M. decorus* that show minimal HSI with *M. guttatus*, most 4x populations of *M. decorus* exhibits an asymmetric barrier with *M. guttatus*, wherein seeds are largely inviable when *M. guttatus* is the maternal donor, northern *M. decorus* exhibit strong, asymmetric inviability when *M. decorus* is the maternal parent, southern *M. decorus* exhibit intermediate -strong asymmetric inviability when *M. guttatus* is the maternal donor. C) representative viable hybrid seeds, D) representative inviable hybrid seeds.

We find substantial variation in HSI throughout the range of *M. decorus*. Northern, southern, and tetraploid clades of *M. decorus* differed significantly from each other in the degree and directionality of HSI with *M. guttatus* (clade effect: χ^2=6.69, *df*=2, *p*=0.035; as well as a clade × cross type interaction: χ^2=135.56, *df*=6, *p*<0.0001; Fig. S6 & S7).

217 Northern *M. decorus* populations tend to produce inviable seeds when they are the
218 maternal donors in crosses with *M. guttatus* (Fig. 2, Table S2), while southern *M. decorus*
219 populations produce more inviable seeds when they are the paternal donor in crosses
220 with *M. guttatus* (Fig. 2). Tetraploids exhibit stronger HSI when they are the paternal
221 donor, although we note two populations with limited HSI (i.e. Fig. 2). In contrast,
222 populations of *M. guttatus* did not drastically differ in their average HSI when crossed
223 with *M. decorus* (Fig. S1).
224

225 **Patterns of hybrid seed inviability show parent of origin effects on growth and**
226 **development**

227 We sought to leverage the diversity of HSI in this system to test for a role of
228 parental conflict in the evolution of HSI using three predictions.

229 *(1) Reciprocal F1 seeds should show differences in size, indicating parent-of-origin effects on*
230 *growth and*

231 *(2) if these parent-of-origin effects on growth cause reproductive isolation, then the degree of*
232 *asymmetry in reciprocal F1 size should correlate with inviability*
233

234 To determine if HSI is associated with parent-of-origin effects on growth, we measured
235 reciprocal F1 seed size and completed a survey of developing hybrid and pure-species
236 seeds for intra-diploid crosses only. HSI was always paired with significant differences
237 in reciprocal F1 hybrid seed size (Table S6; Fig. 3). Northern *M. decorus* produced F1s
238 with larger seeds when they were the maternal donor, while southern *M. decorus*

239 produced larger F1 seeds when they were the paternal donor in crosses with *M. guttatus*

240 (Fig. 3; northern clade crosses: χ^2==296, *df*=3, *p*<0.0001; southern clade crosses: χ^2==298,

241 *df*=3, *p*<0.0001). The level of asymmetry in seed size was correlated with the level of

242 asymmetry in viability (Fig. 3; r^2=-0.69, *df*=22, *p*<0.0001), such that the reciprocal F1 seed

243 that is larger tended to be the seed that was inviable. Thus, HSI is strongly associated

244 with parent-of-origin effects on size; a key prediction of parental conflict.

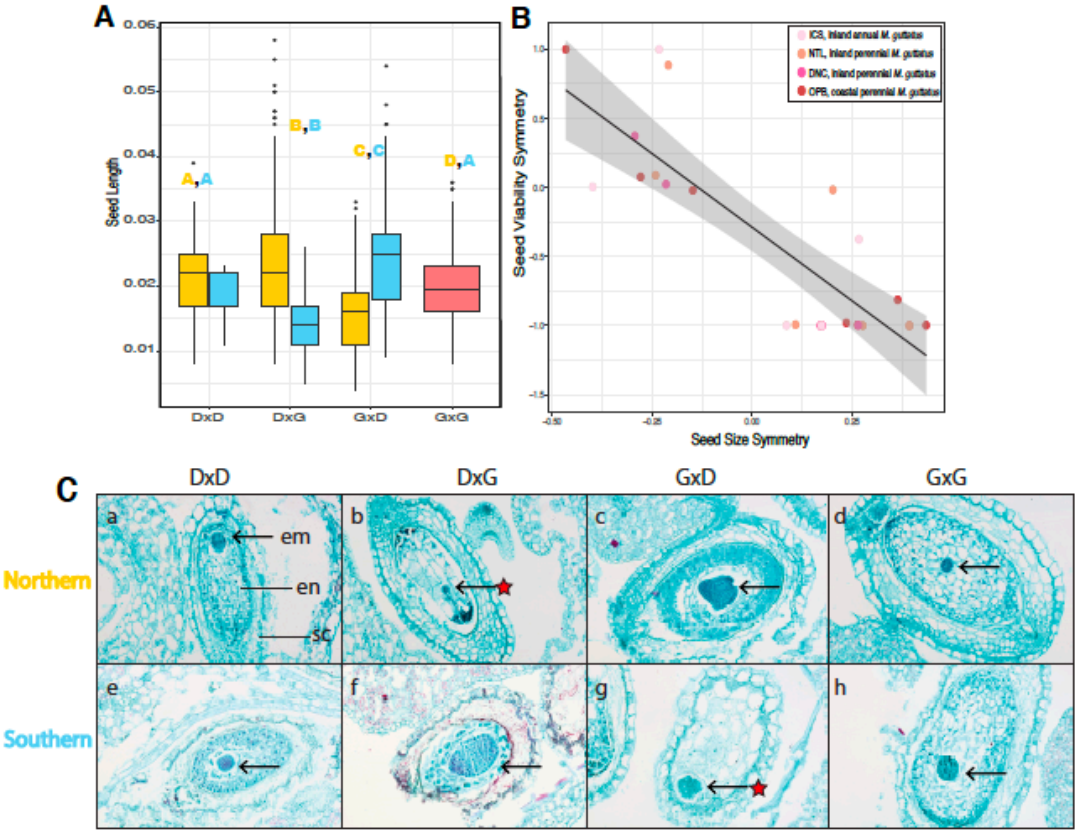

245

246 **Figure 3: A test for conflict using reciprocal F1 seed sizes and symmetries: (A)**
247 **Seed sizes for reciprocal F1s and parents for northern *M. decorus* (yellow) and**
248 **southern *M. decorus* (blue) when crossed to *M. guttatus* (pink). Letters above denote**
249 **significantly different groups, wherein comparable groups are denoted by color. (B)**
250 **Seed viability symmetry between reciprocal F1s as a function of seed size symmetry**
251 **between reciprocal F1s. Color of the points denote the line of *M. guttatus* that was**
252 **used in the cross. The black line indicates the linear regression line of best fit, and**
253 **grey denotes the 95% confidence intervals of the linear regression. (C) Parent of origin**

effects on endosperm proliferation between independent incidences of hybrid seed inviability. (a,d,e,h) Developing seeds of *M. guttatus* ('G') and two genetic clades of *M. decorus* ('D') at 8 days after pollination (DAP). Reciprocal F1s between *M. guttatus* and (b,c) the northern clade of *M. decorus* and (f,g) the southern clade of *M. decorus*. Maternal parent is listed first. Tissues are labeled in panel (a): em=embryo, en=endosperm, sc=seed coat. Arrows denote the location of the developing embryo; red stars indicate that these seeds will eventually become inviable.

To determine if reciprocal F1 size differences were associated with inappropriate development of endosperm we completed developmental surveys of reciprocal F1 seeds from *M. guttatus* crossed to both a focal northern *M. decorus* accession (*IMP*) and a focal southern *M. decorus* accession (*Odell Creek*). Reciprocal F1s between each set of crosses show substantial and parallel parent-of-origin effects on endosperm growth based on seed fate (i.e. whether the seed will remain viable or not; Fig. 3; Fig. S11 & S12). Hybrid seeds that remain viable (e.g. *M. guttatus* × northern *M. decorus* and southern *M. decorus* × *M. guttatus*, with the maternal parent listed first) display a precocious development, with small endosperm cells that are quickly degraded by the embryo (Fig. 3; Fig. S11 & S12), and is almost entirely gone by by 14 Days After Pollination (DAP; Fig. S11 & S12). In contrast, hybrid seeds that will eventually become inviable (i.e. northern *M. decorus* × *M. guttatus* and *M. guttatus* × southern *M. decorus*, with the maternal parent listed first) exhibit a chaotic endosperm growth, producing fewer, but larger and more diffuse endosperm cells (Fig. 3; Fig. S11 & S12). Embryos in this direction of the cross remain small, relative to both parents and the reciprocal hybrid, and are usually degraded by 14 DAP (Fig. 3; Fig. S11 & S12). While the endosperm exhibits parent-of-origin specific growth defects, additional incompatibilities in the embryo cannot be ruled out, as embryo

279 rescues from all crosses (including intraspecific crosses) were generally unsuccessful.
280 Thus, HSI in this system is associated with parent-of-origin specific growth defects of the
281 endosperm that are replicated across independent incidences of HSI, in line with parental
282 conflict.
283
284 *(3) Differences in the strength of conflict between populations (e.g. differences in EBN*
285 *between populations) should predict the degree of reproductive isolation in*
286 *subsequent crosses.*
287 In order to test this prediction, we must first infer EBNs for *M. guttatus* and each clade of
288 *M. decorus*. Other researchers have used mating system and/or ploidy to infer EBNs,
289 however the species we describe here are diploid and exhibit highly outcrossing
290 morphologies (Fig. 5). We therefore use a similar approach to the originators of the
291 concept of EBNs, wherein the EBNs of focal species are inferred from crosses to a
292 common tester line. Predictions can then be made about subsequent crosses between
293 focal species based on these inferred EBNs (Johnson *et al.* 1980, Lin 1984). Using *M.*
294 *guttatus* as our common tester, we predict that northern populations of *M. decorus* likely
295 have a lower EBN (and therefore have experienced a history of weaker conflict) than *M.*
296 *guttatus,* as they are unable to prevent *M. guttatus* paternal alleles from exploiting
297 maternal resources and inducing growth. In contrast, southern populations of *M. decorus*
298 likely have a higher EBN (and therefore have experienced a history of stronger conflict)
299 than *M. guttatus,* as this cross exhibits a paternal excess phenotype when southern *M.*
300 *decorus* is the paternal donor. We next sought to determine whether these designations

301 of EBNs were predictive of reproductive isolation in subsequent crosses using untested
302 intra-diploid and inter-ploidy crosses.
303 First, we crossed all diploid accessions of *M. decorus* to two focal populations; a
304 northern, weaker conflict/ lower EBN *M. decorus* population (*IMP*) and a southern,
305 stronger conflict/ high EBN *M. decorus* population (*Odell Creek*). Secondly, we crossed all
306 tetraploid accessions to each of these focal diploid populations. Given our predicted
307 differences in conflict between diploid clades of *M. decorus,* we can form two distinct
308 predictions: (1) diploid populations of *M. decorus* that exhibit the largest difference in
309 their inferred EBN should exhibit the most HSI, and HSI should be accompanied by
310 reciprocal F1 seed size differences (wherein seeds are larger when northern *M. decorus*
311 are the maternal parents). (2) Tetraploid populations of *M. decorus* should exhibit strong
312 reproductive isolation with low EBN northern *M. decorus* populations (with
313 accompanying reciprocal F1 seed size differences, wherein seeds are larger when
314 northern *M. decorus* is the maternal parent), while high EBN southern *M. decorus*
315 populations should exhibit little or no HSI when crossed to tetraploid *M. decorus* (and
316 minimal seed size differences between reciprocal F1s). We also crossed all four
317 populations of *M. guttatus* used above in all possible combinations to determine if alleles
318 that contribute to HSI were naturally segregating throughout *M. guttatus*.
319 In line with our predictions, we find nearly complete reproductive isolation
320 between northern and southern clades of *M. decorus* (Fig. 4; *IMP* crossed to southern
321 clade: χ^2=12513, *df*=3, *p*<0.0001; *Odell Creek* crossed to northern clade: χ^2==2321.6, *df*=3,

322 p<0.0001), but no reproductive isolation within groups (Fig. S9). In addition, northern *M.*

323 *decorus* show complete reproductive isolation via HSI with tetraploid *M. decorus* (Fig. 4;

324 χ^2=4107, df=3, p<0.0001), but southern *M. decorus* show no HSI with tetraploid *M. decorus*

325 (χ^2==1.69, df=3, p=0.6). We note that geographically and phenotypically distinct

326 populations of *M. guttatus* do not exhibit any signs of HSI (F=0.772, df=1, p=0.39; Fig. S7).

327

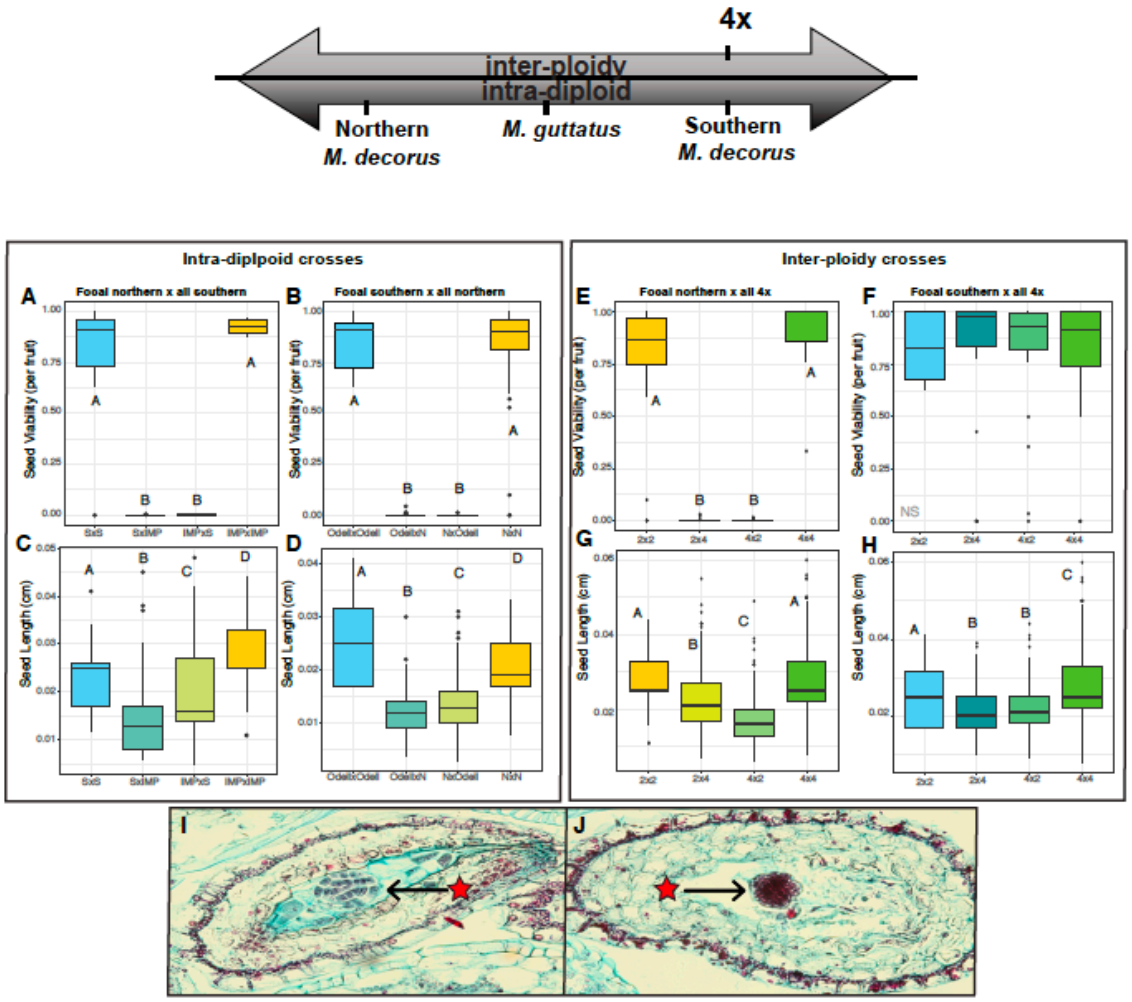

328

329 **Figure 4: Seed viability and size for intra-diploid and inter-ploidy crosses. Top**
330 **arrow denotes a carton representation of the variance in EBN (i.e. our inference of the**
331 **historical level of conflict), where further to the right denotes higher EBN/more**

conflict. Proportion viable seed between (A) a focal northern (e.g. IMP, low conflict) and all southern (high conflict) populations (B) a focal southern (e.g. Odell Creek, high conflict) and all northern (low conflict) populations. Seed sizes for crosses between (C) a focal northern (IMP, low conflict) and all southern (high conflict) populations, (D) a focal southern (e.g. Odell Creek, high conflict) and all northern (low conflict) populations. Crosses between all tetraploid accessions and (E) a focal northern accession (e.g. IMP, low conflict) and (F) a focal southern accession (e.g. Odell Creek, high conflict). Seed sizes for crosses between all tetraploids and (G) a focal northern accession (e.g. IMP, low conflict) and (H) a focal southern accession (e.g. Odell Creek, high conflict). Crosses are denoted with the maternal parent first, S= Southern *M. decorus*, N= Northern *M. decorus*. Letters denote significantly different groups. (I-J) Developing seeds at 8 DAP for crosses between southern and northern clades of *M. decorus* (Odell Creek and IMP, respectively). (I) Odell Creek x IMP, (J) IMP x Odell Creek. Maternal parent is listed first.

In all crosses with strong HSI, reciprocal F1s vary in seed size in the direction predicted by parental conflict (Fig. 4; *IMP* crossed to southern clade: χ^2=79, *df*=3, *p*<0.0001; *Odell Creek* crossed to northern clade: χ^2=301, *df*=3, *p*<0.0001, northern clade *M. decorus* crossed to tetraploids: ; χ^2=349, *df*=3, *p*<0.0001). That is, when higher EBN taxa served as paternal donors F1 seeds were larger, while F1 seeds were smaller when higher EBN taxa severed as the maternal donor. These differences in reciprocal F1 seed size did not occur in crosses within clades (Fig. S9), nor in crosses between taxa with more evenly matched EBNs (e.g. southern *M. decorus* and tetraploid *M. decorus*: *p*=0.7).

In addition, developmental surveys of crosses between southern and northern clades of *M. decorus* exhibited substantial defects in endosperm development in the directions predicted by parental conflict. These defects were more extreme than in crosses between *M. guttatus* and either clade of *M. decorus* (Fig. 3 & 4). When northern *M. decorus* (i.e. *IMP*) was the maternal plant, hybrid seeds produced large and diffuse endosperm cells, while when southern *M. decorus* (i.e. *Odell Creek*) was the maternal

361 parent, hybrid seeds exhibited precociously developing endosperm cells, but hardly any
362 endosperm tissue. Crosses in both directions often had a relatively healthy globular
363 stage embryo at 8 DAP.

364 **Hybrid seed inviability is rapidly evolving within the *M. guttatus* species complex,**
365 **and inferred levels of conflict are positively associated with nucleotide diversity**

366 Despite being each others' closest extant relative, northern and southern clades
367 of *M. decorus* have the most extreme differences in inferred EBN and also the most
368 reproductive isolation via HSI than either do to *M. guttatus.* Given that the northern and
369 southern clades form a monophyletic group that diverged from *M. guttatus* roughly 230
370 kya (Fig. 1), HSI appears to be rapidly evolving in this group. The rapid evolution of
371 alleles associated with parent-of-origin effects on growth is consistent a parental conflict
372 driven arms race of maternal and paternal resource acquisition alleles.

373 The rapid evolution of EBN and HSI in this group suggests that these species
374 vary in some key factor influencing the amount of variance in paternity. Variation in
375 mating system is most commonly used to explain differences in EBN between
376 populations (Brandvain & Haig 2005; Lafon-Placette 2018; Raunsgard *et al.* 2018), yet all
377 species presented here have highly outcrossing morphologies (Fig. 5). We tested
378 whether variation in EBN was associated with genome-wide diversity, as a proxy for
379 effective population size. Using a 4-fold degenerate sites across the genome, we find that
380 inferred EBNs scale positively with genome-wide π, wherein the northern clade of *M.*
381 *decorus* is the least diverse group, and southern *M. decorus* is slightly more diverse than
382 *M. guttatus* (Fig. 5; Table S7). Therefore, differences in inferred conflict between these

383 populations may stem from differences in demographic or life history factors other than

384 mating system.

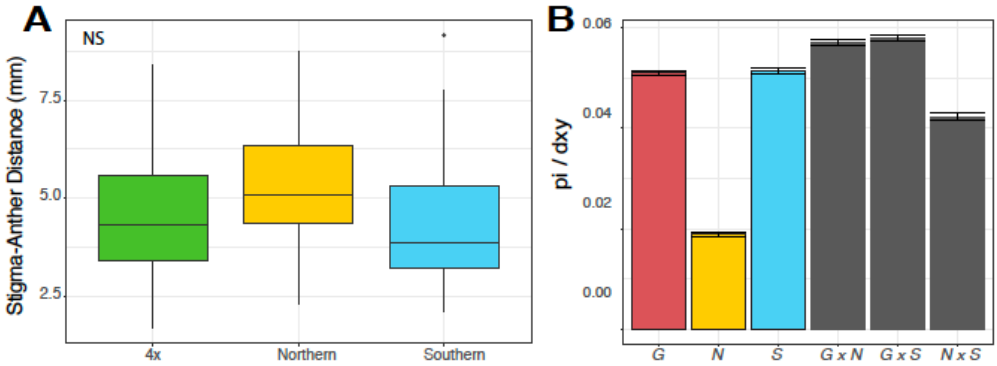

385

386 **Figure 5: Potential correlates of EBN variation in *M. decorus* and *M. guttatus*.**
387 **(A) No difference in the average stigma-anther separation between different clades of**
388 ***M. decorus* (p=0.29), suggesting minimal divergence in mating system evolution, but**
389 **(B) significant variation in genome-wide π between northern and southern clades of**
390 ***M. decorus*, as well as between northern *M. decorus* and *M. guttatus*. Error bars in**
391 **panel (B) represent standard error. G= *M. guttatus*, N= northern *M. decorus*, and S=**
392 **southern *M. decorus*.**
393
394 Overall, we uncovered a cryptic species complex within one of the most

395 commonly studied non-crop plant systems; the *M. guttatus* species complex. *Mimulus*

396 *decorus* likely comprises at least three biological species: a northern diploid, a southern

397 diploid, and at least one tetraploid taxon. These species are largely separated by HSI,

398 and patterns of HSI are conform to the predictions of parental conflict. In addition, HSI

399 is rapidly evolving in this group and EBN is positively associated with genome-wide

400 diversity, highlighting the potential that demographic or life history differences other

401 than mating system may influence the rate of evolution of a parental conflict arms race.

402

403 ## Discussion

404 Here we use a combination of population genomics, common garden
405 experiments, and crossing surveys to describe a cryptic species group- *M. decorus*-
406 nested within the *M. guttatus* species complex. We find that *M. decorus* and *M. guttatus*
407 are largely reproductively isolated via HSI, but the magnitude of reproductive isolation
408 and the direction of the cross that results in inviable hybrid seeds varies throughout the
409 range of *M. decorus.* We leverage variation in HSI between *M. guttatus* and different
410 genetic clades of diploid *M. decorus* to assess whether patterns of HSI can be explained
411 by parental conflict. We find that all three predictions of parental conflict are met in this
412 group, namely: reciprocal F1s show differences in size, the strength of asymmetry in HSI
413 is correlated with asymmetric growth defects between reciprocal F1s, and that inferred
414 EBNs can predict the outcome of crosses. In addition, HSI appears to be rapidly evolving
415 in this group, as the two species that exhibit the most HSI are each others' closest
416 relative. Lastly, the inferred strength of conflict for each clade of *M. decorus* and *M.*
417 *guttatus* scale positively with the level of within-species π, suggesting that demographic
418 or life history factors other than mating system may affect the speed at which parental
419 conflict driven arms races may evolve.

420

421 **Phenotypic and genetic diversity within perennials of the *M. guttatus* species**
422 **complex**

423 Despite morphological similarity, *M. decorus* is genetically unique from and
424 exhibits strong reproductive isolation with *M. guttatus*. Work in the *M. guttatus* species

425 complex has focused on the diversity of annual forms (e.g. Gardner & Macnair 2000;
426 Martin & Willis 2007; Habecker 2012; Peterson *et al.* 2013; Kenney & Sweigart 2016;
427 Ferris & Willis 2018), and differences between annuals and perennials (e.g. Hall & Willis
428 2006; Lowry *et al.* 2009; Peterson *et al.* 2016). Relatively less work has explored diversity
429 within perennials of the complex. Here we find substantial cryptic species diversity
430 within perennials of one of the most well studied, non-crop, plant model systems. Not
431 only do we find that *M. decorus* is a genetically distinct and reproductively isolated
432 species from *M. guttatus*, but it likely represents three reproductively isolated taxa: a
433 diploid northern clade that produces inviable seeds when it is the maternal donor in
434 crosses with *M. guttatus*, a diploid southern clade that produces inviable seeds when it is
435 the paternal donor in crossed with *M. guttatus*, and at least one tetraploid taxon. This
436 highlights a potential difference between annuals and perennials in the *M. guttatus*
437 species complex: annual species generally exhibit both ecological and phenotypic
438 divergence, but very few exhibit substantial post-zygotic reproductive isolation with *M.*
439 *guttatus.* In contrast, *M. decorus* is phenotypically and ecologically very similar to
440 perennial *M. guttatus,* but exhibits relatively strong post-zygotic reproductive isolation.
441 HSI is a common and substantial reproductive barrier between *M. guttatus* and
442 *M. decorus.* This contrasts with other, more geographically restricted intrinsic post-
443 zygotic barriers in this complex (e.g. Sweigart *et al.* 2007; Case & Willis, 2008; Case *et al.*
444 2016; Zuellig & Sweigart 2018a, Zuellig & Sweigart 2018b). Because of its commonality,
445 strength, and the fact that it stops gene flow in the first generation of hybridization, HSI

446 may represent an important barrier in nature. *Mimulus decorus* exhibits striking variation
447 throughout the range in the extent and direction of HSI, which allows us to dissect, in
448 part, the evolutionary drivers of HSI.
449

450 **Patterns of hybrid seed inviability conform to the predictions of parental conflict**

451 We tested three predictions of the role of parental conflict in HSI: (1) reciprocal
452 F1s will show differences in size, (2) size differences between F1s will correlate with the
453 degree of reproductive isolation, and (3) differences in inferred levels of parental conflict
454 are predictive of reproductive isolation in subsequent crosses. We find support for each
455 of these predictions in patterns of HSI between *M. guttatus* and diploid accessions of the
456 morphological variant *M. decorus,* highlighting the potential role of parental conflict in
457 HSI in this group.

458 Evidence for parental conflict in HSI between diploid species pairs has been
459 found in some systems (e.g. *Capsella* Rebernig *et al.* 2015, Lafon-Placette *et al.* 2018;
460 *Arabidopsis* Lafon-Placette *et al.* 2017; wild tomato Roth *et al.* 2017; *peromyscus mice:*
461 Vranna *et al.* 2000; and dwarf hamsters; Brekke *et al.* 2016). In both *Capsella* and *Mimulus,*
462 which show asymmetric inviability, a paternal-excess phenotype appears more lethal
463 (Rebernig *et al.* 2015), which is consistent with inter-ploidy crosses (reviewed in Lafon-
464 Placette & Köhler 2016). In systems with symmetric HSI (e.g. in *Arabidopsis lyrata* and *A.*
465 *arenosa*, Lafon-Placette *et al.* 2017; wild tomato species, Roth *et al.* 2017; and the northern
466 x southern *M. decorus* crosses here), parent-of-origin effects on growth have been shown,

467 although both directions of the cross are often smaller than either parent, perhaps
468 suggesting that in cases of stronger HSI, seeds are aborted earlier. In many of these
469 systems, inviability is caused by malformation of endosperm, rather than an
470 incompatibility manifesting in the embryo (Rebernig *et al.* 2015; Lafon-Placette *et al.* 2017,
471 2018), although in both wild tomatoes and *Mimulus,* HSI tends to produce both
472 malformed endosperm and also early aborting embryos (e.g. Oneal *et al.* 2016; Roth *et al.*
473 2017), which may be related to differences in endosperm developmental programs
474 between *Brassica* and *Solanum*/*Mimulus*.

475 While that patterns of HSI in the *Mimulus guttatus* species complex conform to
476 the predictions of parental conflict, it is possible that evolutionary explanations other
477 than parental conflict could explain HSI. It has been hypothesized that mismatches in
478 small RNAs carried by male and female gametes may result in de-repression of TEs in
479 developing seeds, as imprinted genes are often associated with TEs (Gehring *et al.* 2009;
480 Martienssen 2010). However, unlike parental conflict, the TE hypothesis does not predict
481 asymmetries in growth between reciprocal F1s, as we have found here. In addition, the
482 TE and parental conflict hypotheses are not mutually exclusive; TEs may provide the
483 proximate, molecular mechanism by which genes are imprinted during endosperm
484 development, while parental conflict ultimately drives the evolution of imprinted
485 resource allocation alleles (Köhler *et al.* 2010). A molecular genetic dissection of this
486 incompatibility will be needed to fully understand the proximate and ultimate causes of
487 HSI.

488 **Hybrid seed inviability is rapidly evolving**

489 HSI between northern and southern clades of *M. decorus* highlights the rapidity
490 at which HSI has evolved in this group. These two diploid species are morphologically
491 almost indistinguishable, inhabit similar habitats, and are each others' closest relative.
492 Despite this, HSI between northern and southern *M. decorus* is stronger than HSI
493 between either clade of *M. decorus* and *M. guttatus*. While parental conflict would predict
494 rapid evolution of maternal and paternal resource allocation alleles (Trivers 1974; Haig
495 & Westoby 1989), the variance in the levels of conflict between northern and southern
496 clades of *M. decorus* is curious. Much work on the rate of evolution of HSI due to
497 parental conflict focuses on the role of mating system or ploidy (i.e. Scott *et al.* 1998;
498 Brandvain and Haig 2005; Pennington *et al.* 2008; Rebernig *et al* 2015; Lafon-Placette &
499 Köhler 2016; Lafon-Placette *et al.* 2017; Lafon-Placette *et al.* 2018). Both the southern and
500 northern clades of *M. decorus* are diploid, and exhibit highly outcrossing floral
501 morphologies (i.e. large corollas and significant stigma/anther separation; Fig. 5). One
502 possibility is that differences in conflict may be due to differences in effective population
503 size between *M. guttatus* and each clade of *M. decorus*. This could be caused by a number
504 of factors, including variance in the rates of clonal reproduction, bi-parental inbreeding,
505 or historical population sizes in glacial refugia. Any of these factors would affect the of
506 variance in paternity each clade has experienced historically. Patterns of nucleotide
507 diversity support this hypothesis; northern *M. decorus* is substantially less genetically
508 diverse than either *M. guttatus* or southern *M. decorus,* while southern *M. decorus* is

509 slightly more genetically diverse than *M. guttatus*. However, more detailed demographic
510 and population genomic analyses are needed to investigate this hypothesis further.
511

512 Acknowledgements

513 We thank Shivam Dave for help with seed counting, and Madison Zamora for
514 assistance with field work. Miguel Flores provided valuable expertise and help with
515 flow cytometry, and chromosomal squashes were only possible with the patient help of
516 Michael Windham. We thank Yaniv Brandvain and Josh Puzey for access to the whole
517 genome re-sequencing data for several accessions of *M. guttatus.* We are deeply grateful
518 to members of the Willis and Matute lab, particularly Daniel Matute, who provided
519 useful comments on this manuscript. We also thank those who provided insightful
520 comments during the 2019 Gordon Speciation Conferences in Ventura, CA. This project
521 was funded from NSF grants EF-0328636 and EF-0723814 to JHW, a DDIG (DEB-
522 1501758), ASN Student research award and SSE student research award to JMC. JMC
523 was also funded through the Duke Graduate School via the Myra and William Waldo
524 Boone fellowship, the Duke Biology Department, and NIGMS grant R01GM121750 to
525 Daniel Matute. Duke BioCore provided support for MWB. The authors declare no
526 conflict of interest.
527

Data Accessibility

All data will be made publically available upon the acceptance of this manuscript.

Author Contributions

JMC designed the project, collected data, performed all analyses, and wrote the manuscript. MWB helped with data collection. JHW contributed substantially to the ideas presented here and the project design.

References

Arnegard, M. E., McGee, M. D., Matthews, B., Marchinko, K. B., Conte, G. L., Kabir, S., … Schluter, D. (2014). Genetics of ecological divergence during speciation. *Nature*, *511*, 307–311.

Barnard-Kubow, K. B., & Galloway, L. F. (2017). Variation in reproductive isolation across a species range. *Ecology and Evolution*, (August), 1–11.

Bates, D., Maechler M., Bolker B., Walker S. (2015). Fitting Linear Mixed-Effects Models Using lme4. Journal of Statistical Software, 67(1), 1-48.

Bomblies, K., & Weigel, D. (2007). Hybrid necrosis: autoimmunity as a potential gene-flow barrier in plant species. *Nature Reviews. Genetics*, *8*(5), 382–393.

Bracewell, R. R., Bentz, B. J., Sullivan, B. T., & Good, J. M. (2017). Rapid neo-sex chromosome evolution and incipient speciation in a major forest pest. *Nature Communications*, *8*(1), 1593.

Bradshaw, H., & Schemske, D. W. (2003). Allele substitution at a flower colour locus produces a pollinator shift in monkeyflowers. *Nature*, *44*(3), 138–147.

Brandvain, Y., & Haig, D. (2005). Divergent mating systems and parental conflict as a barrier to hybridization in flowering plants. *The American Naturalist*, *166*(3), 330–338.

Brandvain, Y., Kenney, A. M., Flagel, L. E., Coop, G., & Sweigart, A. L. (2014). Speciation and Introgression between Mimulus nasutus and Mimulus guttatus. *PLoS Genetics*, *10*(6).

Brekke, Th. D., & Good, J. M. (2014). Parent-of-origin growth effects and the evolution of hybrid inviability in dwarf hamsters. *Evolution*, *68*(11), 3134–3148.

Brekke, T. D., Henry, L. a., & Good, J. M. (2016). Genomic imprinting, disrupted placental expression, and speciation. *Evolution*, *3*(Haig 1996), 1–14.

Cailleau, A., Grimanelli, D., Blanchet, E., Cheptou, P.-O., & Lenormand, T. (2018). Dividing a Maternal Pie among Half-Sibs: Genetic Conflicts and the Control of Resource Allocation to Seeds in Maize. *The American Naturalist*, *192*(5), 000–000.

Case, A. L., Finseth, F. R., Barr, C. M., & Fishman, L. (2016). Selfish evolution of cytonuclear hybrid incompatibility in Mimulus. *Proceedings of the Royal Society B*, *283*.

Case, A. L., & Willis, J. H. (2008). Hybrid male sterility in Mimulus (Phrymaceae) is associated with a geographically restricted mitochondrial rearrangement. *Evolution*, *62*(5), 1026–1039.

Castillo, D. M., & Moyle, L. C. (2012). Evolutionary Implications of Mechanistic Models of TE-Mediated Hybrid Incompatibility. *International Journal of Evolutionary Biology*, *2012*, 698198.

Catchen, J., Hohenlohe, P. a., Bassham, S., Amores, A., & Cresko, W. a. (2013). Stacks: An analysis tool set for population genomics. *Molecular Ecology*, *22*(11), 3124–3140.

Charnov, E. L., & Hutchinson, G. E. (1979). Population Biology Simultaneous hermaphroditism and sexual selection, *76*(5), 2480–2484.

Comai, L. (2005). The advantages and disadvantages of being polyploid. *Nature Reviews*, *6*(11), 836–846.

Coughlan, J. M., & Willis, J. H. (2018). Dissecting the role of a large chromosomal inversion in life history divergence throughout the Mimulus guttatus species complex. *Molecular Ecology*, (April), 1-15.

Danecek, P., Auton, A., Abecasis, G., Albers, C. A., Banks, E., Depristo, M. A., … Vcf, T. (2011). The variant call format and VCFtools, *27*(15), 2156–2158.

Ferris, K. G., & Willis, J. H. (2018). Differential Adaptation to a Harsh Granite Outcrop Habitat between Sympatric. *Evolution*, *72*(6), 1225–1241.

Fishman, L., Kelly, A. J., & Willis, J. H. (2002). Minor Quantitative Trait Loci Underlie Floral Traits Associated with Mating System Divergence in Mimulus. *Evolution*, *56*(11), 2138–2155.

Fishman, L., & Kelly, J. K. (2015). Centromere-associated meiotic drive and female fitness variation in *Mimulus*. *Evolution*, *69*, 1208–1218.

Fitzpatrick, B. M. (2004). Rates of evolution of hybrid inviability in birds and mammals. *Evolution*, *58*(8), 1865–1870.

Fox J. & Weisberg S. (2011). An {R} Companion to Applied Regression, Second Edition. Thousand Oaks CA: Sage.

Friedman, J., Twyford, A. D., Willis, J. H., & Blackman, B. K. (2015). The extent and genetic basis of phenotypic divergence in life history traits in Mimulus guttatus. *Molecular Ecology*, *24*(1), 111–122.

Galbraith, D. W., Lambert, G. M., Macas, J., & Dolezel, J. (2001). Analysis of nuclear DNA content and ploidy in higher plants. *Current Protocols in Cytometry*, *Chapter 7*, Unit 7.6.

Gardner, M., & Macnair, M. (2000). Factors affecting the co-existence of the serpentine endemic Mimulus nudatus Curran and it presumed progenitor, Mimulus guttatus Fischer ex DC. *Biological Journal of the Linnean Society*, *69*, 443–459.

Garner, A. G., Kenney, A. M., Fishman, L., & Sweigart, A. L. (2016). Genetic loci with parent of origin effects cause hybrid seed lethality between Mimulus species. *New Phytologist*, *211*, 319–331.

Gehring, M., Bubb, K. L., & Henikoff, S. (2009). Extensive Demethylation of Repetitive. *Science*, *324*, 1447–1451.

Grant, A. L. (1924). A monograph of the genus Mimulus. *Annals of the Missouri Botanical Garden*, *11*(2), 99–388.

Habecker, N. M. (2012). *Ecogeographical and intrinsic postzygotic isolation between Mimulus glaucescens and Mimulus guttatus* (Masters thesis). Retrieved from California State University Chico repository.

Haig, D. (1997). Parental antagonism, relatedness asymmetries, and genomic imprinting. *Proceedings of the Royal Society B: Biological Sciences*, *264*(1388), 1657–1662.

Haig, D., & Mark Westoby. (1989). Parent-specific gene expression and the triploid endosperm. *American Naturalist*, *134*(1), 147–155.

Hall, M. C., & Willis, J. H. (2006). Divergent selection on flowering time contributes to local adaptation in Mimulus guttatus populations. *Evolution*, *60*(12), 2466–2477.

Johnston, S. a., den Nijs, T. P. M., Peloquin, S. J., & Hanneman, R. E. (1980). The significance of genic balance to endosperm development in interspecific crosses. *Theoretical and Applied Genetics*, *57*(1), 5–9.

Kenney, A. M., Sweigart, A. L., & Kenney, A. M. (2016). Reproductive isolation and introgression between sympatric Mimulus species. *Molecular Ecology*, *25*, 2499–2517.

Korneliussen, T. S., Albrechtsen, A., & Nielsen, R. (2014). Open Access ANGSD : Analysis of Next Generation Sequencing Data, 1–13.

Köhler, C., & Weinhofer-Molisch, I. (2010). Mechanisms and evolution of genomic imprinting in plants. *Heredity*, *105*(1), 57–63.

Köhler, C., Mittelsten Scheid, O., & Erilova, A. (2010). The impact of the triploid block on the origin and evolution of polyploid plants. *Trends in Genetics*, *26*(3), 142–148.

Kradolfer, D., Wolff, P., Jiang, H., Siretskiy, A., & Köhler, C. (2013). An imprinted gene underlies postzygotic reproductive isolation in arabidopsis thaliana. *Developmental Cell*, *26*(5), 525–535.

Kreuger, F. Trim Galore! 0.3. 7 In.

Lafon-Placette, C., Hatorangan, M. R., Steige, K. A., Cornille, A., Lascoux, M., Slotte, T., & Köhler, C. (2018). Paternally expressed imprinted genes associate with hybridization barriers in Capsella. *Nature Plants*.

Lafon-Placette, C., Johannessen, I. M., Hornslien, K. S., Ali, M. F., Bjerkan, K. N., Bramsiepe, J., … Köhler, C. (2017). Endosperm-based hybridization barriers explain the pattern of gene flow between *Arabidopsis lyrata* and *Arabidopsis arenosa* in Central Europe. *Proceedings of the National Academy of Sciences*, 201615123.

Lafon-Placette, C., & Köhler, C. (2016). Endosperm-based postzygotic hybridization barriers: Developmental mechanisms and evolutionary drivers. *Molecular Ecology*, 2620–2629.

Li, H., & Durbin, R. (2009). Fast and accurate short read alignment with Burrows-Wheeler transform. *Bioinformatics*, *25*(14), 1754–1760.

Li, H., Handsaker, B., Wysoker, A., Fennell, T., Ruan, J., Homer, N., Marth, G., Abecasis, G., Durbin, R. (2009). The Sequence Alignment/Map format and SAMtools. *Bioinformatics*, *25*(16), 2078–2079.

Lin, B. Y. (1984). Ploidy barrier to endosperm development in maize. *Genetics*, *107*(1), 103–115.

Lowry, D. B., Hall, M. C., Salt, D. E., & Willis, J. H. (2009). Genetic and physiological basis of adaptive salt tolerance divergence between coastal and inland Mimulus guttatus. *The New Phytologist*, *183*(3), 776–788.

Lowry, D. B., Modliszewski, J. L., Wright, K. M., Wu, C. A., & Willis, J. H. (2008). The strength and genetic basis of reproductive isolating barriers in flowering plants. *Philosophical Transactions of the Royal Society B*, *363*(1506), 3009–3021.

Lowry, D.B., Sobel J.M., Angert A.L., Ashman T., Baker R.L., Blackman, B.K., Brandvain, Y., Byers K. J. R. P., Cooley A.M., Coughlan, J.M., Dudash, M.R., Fenster, C.B., Ferris, K. G., Fishman, L., Friedman, J., Grossenbacher, D.L., Holeski, L.M., Ivey, C.T., Kay, K.M., Koelling, V.A., Kooyers, N.J., Murren, C.J., Muir, C.D., Nelson, T.C, Peterson, M.L., Puzey, J.R., Rotter, M.C., Seemann, J.R., Sexton, J.P., Sheth, S.N., Streisfeld, M.A., Sweigart, A.L., Twyford, A.D., Vallejo-Marín, M, Willis, J.H., Wu, C.A., Yuan, Y-W. The case for the continued use of the genus name *Mimulus* for all monkeyflowers. Taxon *in press*.

Lynch, M., & Force, A. G. (2000). The Origin of Interspecific Genomic Incompatibility via Gene Duplication. *The American Naturalist*, *156*(6), 590–605.

Martienssen, R. A. (2010). Heterochromatin, small RNA and post-fertilization dysgenesis in allopolyploid and interploid hybrids of Arabidopsis. *New Phytologist*, *186*(1), 46–53.

Martin, N. H., & Willis, J. H. (2010). Geographical variation in postzygotic isolation and its genetic basis within and between two Mimulus species. *Philosophical Transactions of the Royal Society B: Biological Sciences*, *365*(1555), 3261–3261.

Martin, N. H., & Willis, J. H. (2007). Ecological divergence associated with mating system causes nearly complete reproductive isolation between sympatric Mimulus species. *Evolution; International Journal of Organic Evolution*, *61*(1), 68–82.

McKenna, A., Hanna, M., Banks, E., Sivachenko, A., Cibulskis, K., Kerntsky, A., … DePristo, M. A. (2010). The Genome Analysis Toolkit: A MapReduce framework for analysing next-generation DNA sequencing data. *Genome Research*, *20*, 1297–1303.

Nesom, G. L. (2012). Taxonomy of erythranthe sect. simiolus (phrymaceae) in the usa and mexico. *Phytoneuron*, (1978).

Nosil, P., Vines, T. H., & Funk, D. J. (2005). Reproductive isolation casued by natural selection against immigrants from divergent habitats. *Evolution*, *59*, 705–719.

Oneal, E., Willis, J. H., & Franks, R. G. (2016). Disruption of endosperm development is a major cause of hybrid seed inviability between Mimulus guttatus and Mimulus nudatus. *New Phytologist*, *210*, 1107–1120.

Paradis E. & Schliep K. 2018. ape 5.0: an environment for modern phylogenetics and evolutionary analyses in R. Bioinformatics 35: 526-528.

Pennington, P. D., Costa, L. M., Gutierrez-Marcos, J. F., Greenland, A. J., & Dickinson, H. G. (2008). When genomes collide: Aberrant seed development following maize interploidy crosses. *Annals of Botany*, *101*(6), 833–843.

Peterson, M. L., Kay, K. M., & Angert, A. L. (2016). The scale of local adaptation in Mimulus guttatus : comparing life history races , ecotypes , and populations. *New Phytologist*, *211*, 345–356.

Peterson, M. L., Rice, K. J., & Sexton, J. P. (2013). Niche partitioning between close relatives suggests trade-offs between adaptation to local environments and competition. *Ecology and Evolution*, *3*(3), 512–522.

Prager, E. M., & Wilson, a. C. (1975). Slow evolutionary loss of the potential for interspecific hybridization in birds: a manifestation of slow regulatory evolution. *Proceedings of the National Academy of Sciences*, *72*(1), 200–204.

R Core Team (2017). R: A language and environment for statistical computing. R Foundation for Statistical Computing, Vienna, Austria. URL https://www.R-project.org/.

Ramsey, J., Bradshaw, H. D., & Schemske, D. W. (2003). Components of reproductive isolation between the monkeyflowers Mimulus lewisii and M. cardinalis (Phrymaceae). *Evolution*, *57*(7), 1520–1534.

Raunsgard, A., Opedal, Ø. H., Ekrem, R. K., Wright, J., Bolstad, G. H., Armbruster, W. S., & Pélabon, C. (2018). Intersexual conflict over seed size is stronger in more outcrossed populations of a mixed-mating plant. *Proceedings of the National Academy of Sciences*, 201810979.

Rebernig, C. a., Lafon-Placette, C., Hatorangan, M. R., Slotte, T., & Köhler, C. (2015). Non-reciprocal Interspecies Hybridization Barriers in the Capsella Genus Are Established in the Endosperm. *PLOS Genetics*, *11*(6), e1005295.

Roth, M., Florez-Rueda, A. M., Griesser, S., Paris, M., & Städler, T. (2017). Incidence and developmental timing of endosperm failure in postzygotic isolation between wild tomato lineages. *Annals of Botany*, (January), 1–12.

Schliep K.P. 2011. phangorn: phylogenetic analysis in R. Bioinformatics, 27(4) 592-593

Schneider, C. a., Rasband, W. S., & Eliceiri, K. W. (2012). NIH Image to ImageJ: 25 years of image analysis. *Nature Methods*, *9*(7), 671–675.

Scott, R. J., Spielman, M., Bailey, J., & Dickinson, H. G. (1998). Parent-of-origin effects on seed development in Arabidopsis thaliana. *Development (Cambridge, England)*, *125*(October 2014), 3329–3341.

Selby, J. P., & Willis, J. H. (2018). Major QTL controls adaptation to serpentine soils in Mimulus guttatus, (August), 5073–5087.

Sicard, A., Kappel, C., Josephs, E. B., Lee, Y. W., Marona, C., Stinchcombe, J. R., … Lenhard, M. (2015). Divergent sorting of a balanced ancestral polymorphism underlies the establishment of gene-flow barriers in Capsella. *Nature Communications*, *6*, 7960.

Sweigart, A. L., Fishman, L., & Willis, J. H. (2006). A simple genetic incompatibility causes hybrid male sterility in mimulus. *Genetics*, *172*(4), 2465–2479.

Sweigart, A. L., Mason, A. R., & Willis, J. H. (2007). Natural variation for a hybrid incompatibility between two species of mimulus. *Evolution*, *61*(1), 141–151.

Tiffin, P., Olson, M. S., & Moyle, L. C. (2001). Asymmetrical crossing barriers in angiosperms. *Proceedings. Biological Sciences / The Royal Society*, *268*(1469), 861–867.

Toll, K., & Willis, J. H. (2019). Hybrid inviability and differential submergence tolerance drive habitat segregation between two congeneric monkey fl owers, *99*(12), 2776–2786.

Trivers, R. L. (1974). Parent-Offspring Conflict. *American Zoology*, *14*(1), 249–264.

Twyford, A. D., & Friedman, J. (2015). Adaptive divergence in the monkey flower Mimulus guttatus is maintained by a chromosomal inversion. *Evolution*, *69*(9), 1476–1486.

Twyford, A. D., Streisfeld, M. A., Lowry, D. B., & Friedman, J. (2015). Genomic studies on the nature of species: Adaptation and speciation in Mimulus. *Molecular Ecology*, *24*(11), 2601–2609.

Vrana, P. B. (2007). Genomic Imprinting As a Mechanism of Reproductive Isolation in Mammals, *88*(1), 5–23.

Vrana, P. B., Fossella, J. a, Matteson, P., del Rio, T., O'Neill, M. J., & Tilghman, S. M. (2000). Genetic and epigenetic incompatibilities underlie hybrid dysgenesis in Peromyscus. *Nature Genetics*, *25*(1), 120–124.

White, R. A., & Turner, M. D. (2012). The Anatomy and Occurrence of Foliar Nectaries in Cyathea (Cyatheaceae). *American Fern Journal*, *102*(2), 91–113.

Willi, Y. (2013). The Battle of the Sexes over Seed Size: Support for Both Kinship Genomic Imprinting and Interlocus Contest Evolution. *The American Naturalist*, *181*(6), 787–798.

Wilson, a. C., Maxson, L. R., & Sarich, V. M. (1974). Two types of molecular evolution: evidence from studies of interspecific hybridization. *Proceedings of the National Academy of Sciences of the United States of America*, *71*(7), 2843–2847.

Wolff, P., Jiang, H., Wang, G., Santos-González, J., & Köhler, C. (2015). Paternally expressed imprinted genes establish postzygotic hybridization barriers in *Arabidopsis thaliana*. *ELife*, *4*, 1–14.

Wright, K. M., Lloyd, D., Lowry, D. B., Macnair, M. R., & Willis, J. H. (2013). Indirect evolution of hybrid lethality due to linkage with selected locus in *Mimulus guttatus*. *PLoS Biology*, *11*(2), e1001497.

Wu, C. A., Lowry, D. B., Cooley, a M., Wright, K. M., Lee, Y. W., & Willis, J. H. (2008). Mimulus is an emerging model system for the integration of ecological and genomic studies. *Heredity*, *100*(2), 220–230.

Zechner, U., Shi, W., Hemberger, M., Himmelbauer, H., Otto, S., Orth, a., … Fundele, R. (2004). Divergent genetic and epigenetic post-zygotic isolation mechanisms in Mus and Peromyscus. *Journal of Evolutionary Biology*, *17*(2), 453–460.

Zuellig, M. P., & Sweigart, A. L. (2018)a. A two-locus hybrid incompatibility is widespread, polymorphic, and active in natural populations of Mimulus. *Evolution*, 1–12.

Zuellig, M. P., & Sweigart, A. L. (2018)b. Gene duplicates cause hybrid lethality between sympatric species of Mimulus. *PLoS*, *14*(4), e1007130.

Figure Captions

Figure 1: Phenotypic and genetic description of focal members of the *M. guttatus* species complex. (A) Geographic sampling of genetic samples from *M. guttatus* and *M. decorus.* Inland versus coastal perennials were not distinguished in the previous study and are

793 thus both indicated by darker pink points in this panel. (B) Legend of the colors used to
794 denote each species (C) NJ tree constructed using 4-fold degenerate sites and rooted
795 using *M. dentilobus*. (D) PCA of 15 morphological characteristics for perennials within
796 the *M. guttatus* species complex, as well as perennial *M. tilingii* and annual *M. guttatus.*
797 Trait codes as follows: FT- days to first flower, FN- node of first flower, ST-stem
798 thickness, CW- corolla width, TL- tube length, CL- corolla length, LL- leaf length, LW-
799 leaf width, IL1- first internode length, IL2- second internode length, NS- number of
800 stolons, SL- stolon length, SW- stolon width, SBL- side branch length, NSB- number of
801 side branches. (E) PCA of re-sequencing data for focal members of the *M. guttatus*
802 species complex. In both PCAs the percent of total variance explained by that PC is
803 indicated in parentheses.

804

805 **Figure 2:** Geographic distribution of hybrid seed inviability between *M. decorus* and *M.*
806 *guttatus*. (A) Sampling locales of 19 populations of *M. decorus* that were crossed to four
807 *M. guttatus* populations reciprocally. Points are colored as in Fig.1, but points which are
808 lighter in hue are populations that exhibit limited reproductive isolation with *M.*
809 *guttatus*. (B) Crossing patterns for four populations of *M. decorus,* representing the four
810 main crossing phenotypes observed (from top left to bottom right): 2 populations of
811 tetraploid *M. decorus* that show minimal HSI with *M. guttatus,* most 4x populations of *M.*
812 *decorus* exhibits an asymmetric barrier with *M. guttatus*, wherein seeds are largely
813 inviable when *M. guttatus* is the maternal donor, northern *M. decorus* exhibit strong,

814 asymmetric inviability when *M. decorus* is the maternal parent, southern *M. decorus*
815 exhibit intermediate -strong asymmetric inviability when *M. guttatus* is the maternal
816 donor. C) representative viable hybrid seeds, D) representative inviable hybrid seeds.

817

818 **Figure 3:** A test for conflict using reciprocal F1 seed sizes and symmetries: (A) Seed sizes
819 for reciprocal F1s and parents for northern *M. decorus* (yellow) and southern *M. decorus*
820 (blue) when crossed to *M. guttatus* (pink). Letters above denote significantly different
821 groups, wherein comparable groups are denoted by color. (B) Seed viability symmetry
822 between reciprocal F1s as a function of seed size symmetry between reciprocal F1s.
823 Color of the points denote the line of *M. guttatus* that was used in the cross. The black
824 line indicates the linear regression line of best fit, and grey denotes the 95% confidence
825 intervals of the linear regression. (C) Parent of origin effects on endosperm proliferation
826 between independent incidences of hybrid seed inviability. (a,d,e,h) Developing seeds of
827 *M. guttatus* ('G') and two genetic clades of *M. decorus* ('D') at 8 days after pollination
828 (DAP). Reciprocal F1s between *M. guttatus* and (b,c) the northern clade of *M. decorus* and
829 (f,g) the southern clade of *M. decorus.* Maternal parent is listed first. Tissues are labeled
830 in panel (a): em=embryo, en=endosperm, sc=seed coat. Arrows denote the location of the
831 developing embryo; red stars indicate that these seeds will eventually become inviable.

832

833 **Figure 4:** Seed viability and size for intra-diploid and inter-ploidy crosses. Top arrow
834 denotes a carton representation of the variance in EBN (i.e. our inference of the historical
835 level of conflict), where further to the right denotes higher EBN/more conflict.
836 Proportion viable seed between (A) a focal northern (e.g. IMP, low conflict) and all
837 southern (high conflict) populations (B) a focal southern (e.g. Odell Creek, high conflict)
838 and all northern (low conflict) populations. Seed sizes for crosses between (C) a focal
839 northern (IMP, low conflict) and all southern (high conflict) populations, (D) a focal
840 southern (e.g. Odell Creek, high conflict) and all northern (low conflict) populations.
841 Crosses between all tetraploid accessions and (E) a focal northern accession (e.g. IMP,
842 low conflict) and (F) a focal southern accession (e.g. Odell Creek, high conflict). Seed
843 sizes for crosses between all tetraploids and (G) a focal northern accession (e.g. IMP, low
844 conflict) and (H) a focal southern accession (e.g. Odell Creek, high conflict). Crosses are
845 denoted with the maternal parent first, S= Southern *M. decorus*, N= Northern *M. decorus.*
846 Letters denote significantly different groups. (I-J) Developing seeds at 8 DAP for crosses
847 between southern and northern clades of *M. decorus* (Odell Creek and IMP,
848 respectively). (I) Odell Creek x IMP, (J) IMP x Odell Creek. Maternal parent is listed first.
849

850 **Figure 5:** Potential correlates of EBN variation in *M. decorus* and *M. guttatus.* (A) No
851 difference in the average stigma-anther separation between different clades of *M. decorus*
852 (p=0.29), suggesting minimal divergence in mating system evolution, but (B) significant
853 variation in genome-wide π between northern and southern clades of *M. decorus,* as well

as between northern *M. decorus* and *M. guttatus.* Error bars in panel (B) represent standard error. G= *M. guttatus,* N= northern *M. decorus,* and S= southern *M. decorus.*

875 # STAR Methods

876 ## CONTACT FOR REAGENT AND RESOURCE SHARING

877 Further information and requests for resources and reagents should be directed to and will
878 be fulfilled by the Lead Contact, Jennifer Coughlan (jcoug@email.unc.edu)

879

880 ## EXPERIMENTAL MODEL AND SUBJECT DETAILS

881 ### The *Mimulus guttatus* species complex

882 The *Mimulus guttatus* species complex is a morphologically, ecologically, and
883 genetically diverse group (Wu *et al.* 2008; Twyford *et al.* 2015). The species complex is
884 home to several known annual species, as well as many perennial morphological
885 variants. In fact, *M. guttatus* itself comprises several morphological variants, including
886 two inland perennials (*M. guttatus sensu stricto,* and *M. decorus*), and a coastal perennial
887 (*M. grandis*), that are phenotypically differentiated by subtle distinctions in corolla
888 length, leaf shape, and the types, densities and locations of trichomes (Grant 1924;
889 Nesom 2012). We refer to these as inland *M. guttatus*, *M. decorus*, and coastal *M. guttatus*,
890 respectively. *Mimulus tilingii* is the most divergent perennial species, and represents its
891 own species complex (Grant 1924; Nesom 2012; Garner *et al.* 2016). Little is known about
892 the phenotypic, genetic relationships and reproductive barriers between
893 morphologically described perennials of the *M. guttatus* species complex.

894 **Plant rearing and common garden conditions**

895 For the phenotypic survey and crossing survey described below, we grew plants
896 in a common garden in the Duke Greenhouses under long day conditions (18h days, 21C
897 days/18C nights). Between 1-5 maternal families with 5 replicates/family for each of six
898 populations of annual *M. guttatus*, seven populations of coastal perennial *M. guttatus,* 16
899 populations of inland perennial *M. guttatus*, 18 populations of *M. decorus* and seven
900 populations of *M. tilingii* were grown. Seeds were first cold stratified for one week on
901 moist Fafard 4P soil then transferred to the greenhouses. Germinants were transplanted
902 on the day of germination and phenotyped on the day of first flower.

903
904
905 **METHOD DETAILS**
906

907 **Phenotypic survey**

908 To assess the degree of phenotypic differentiation among members of the *M.*
909 *guttatus* species complex, we use data from the common garden experiment described in
910 Coughlan & Willis (2018). Briefly, on the day of first flower, we measured 15
911 morphological traits (days from germination to first flower, node of first flower, total
912 corolla length, corolla tube length, corolla width, stem thickness, leaf length and width,
913 internode length between the cotyledons and first true leaf, internode length between
914 the first and second pair of true leaves, the number of stolons, length of the longest
915 stolon, width of the longest stolon, number of side branches, length of the longest side

916 branch). We also assessed stigma-anther separation on individuals from each maternal
917 family of *M. decorus.*

918 **Population genetics survey**

919 To determine the genetic relationship among perennials of the *M. guttatus*
920 species complex, we leveraged previously published whole genome re-sequencing and
921 GBS data with new re-sequence data for several members of the *M. guttatus* species
922 complex (outlined in Supplemental Table 1). This sample includes genomes from 222
923 accessions: 199 *M. guttatus (*113 perennials, 74 annuals, and 12 individuals of unknown
924 or intermediate life history), two additional perennial species, including 15 *M. decorus*
925 and two *M. tilingii* accessions, and five additional annual *M. nasutus* accessions. We also
926 included a single accession of *M. dentilobus* as the outgroup. For the whole-genome re-
927 sequencing data, all genomic DNA was extracted from young bud or leaf tissue, and
928 150bp, paired-end read Illumina libraries were made by either the Duke Sequencing
929 facility or by using Illumina Nextera DNA kit (described in Puzey *et al.* 2017). Libraries
930 were then sequenced on either an Illumina 2500 or 4000 platforum to an average of 15x
931 coverage (range: 3.3x-51.5x Supplemental Table 1).

932

933 ***Determining genome size and ploidy***

934 We performed a combination of flow cytometry and chromosome squashes to assess
935 ploidy variation within *M. decorus*. We surveyed 1-2 individuals per population of *M.*
936 *decorus* to determine total genomic content using flow cytometry (outlined in Galbraith

937 *et al.* 1997). Briefly, we chopped freshly collected, young leaf tissue in Cystain UV Precise
938 P buffer for each individual, as well as an internal standard, *Arabidopsis thaliana* (2n=2x,
939 2C=0.431pg; Schmuths *et al.* 2004). Samples in buffer were filtered through a 40 μm, then
940 20 μm pore-sized nylon mesh. Shortly before analysis, we added 0.1mg/ml of 4',6-
941 diamidino-2-phenylindole (DAPI). Nuclei stained for at least ten minutes before being
942 run on a Becton Dickinson LSRII flow cytometer. Total DNA content was calculated by
943 the following equation:

944 $$\text{2C DNA content (pg DNA)} = \frac{sample\ G1\ peak\ mean}{standard\ G1\ peak\ mean}\ x\ standard\ 2C\ DNA\ content$$

945

946 Total genomic content ranged from 2C= 0.61- 3.06 pg (Supplemental Figure 3). To
947 confirm that larger genomic content corresponded with changes in ploidy, we
948 performed meiotic chromosomal squashes on select populations that spanned the range
949 of genome size (0.67pg, 1.06pg, 1.22 pg, 1.43 pg, 2 pg, and 2.96 pg). From these squashes,
950 all individuals with genome sizes <1.22pg were found to be diploid (2n=2x=14), while all
951 individuals with genomes between 1.43-2.96pg were found to be tetraploid (2n=4x=28).
952 As meiotic chromosomal squashes were not possible for all accessions due to constraints
953 of both labor and plant material, we inferred ploidy for the remaining samples based on
954 these ranges, wherein individuals with a genome size of 1.2pg or less were classified as
955 diploid, and those with a genome size of 1.43 or higher were classified as tetraploid.
956 Two accessions (HJA and Kink Creek) exhibited genome sizes that were intermediate to
957 our cutoffs (1.25pg and 1.41pg, respectively). However, these accessions tightly clustered

958 with northern diploids in our genomic PCA and are in close geographic proximity to all
959 other northern diploids. In contrast, almost all of the tetraploids sampled were from
960 more northerly latitudes and formed a separate genetic cluster in our PCA analysis. We
961 therefore treat these two accessions as northern diploids. We note that our results do not
962 qualitatively change whether these two samples are retained or omitted from analyses.
963

964 **Crossing survey between *M. guttatus* and *M. decorus***

965 To assess hybrid seed inviability between perennials in this group we crossed 19
966 populations of *M. decorus* to an average of 4 populations of *M. guttatus* reciprocally, as
967 well as within population crosses, with an average of 13 replicates per cross (ranging
968 from 2-37 replicate crosses, totaling 1020 fruits; Supplemental Table 1 & 2). The 19
969 populations of *M. decorus* represented all three genetic clades, including: five northern
970 *M. decorus* populations, two southern *M. decorus* populations, and twelve tetraploid
971 populations. The four populations of *M. guttatus* that were used maximize the
972 phenotypic and genetic diversity of the species and include one annual, two inland
973 perennials, and one coastal perennial population. Due to the sheer number of crosses,
974 individuals were used for multiple crosses and acted as both seed and pollen parents.
975 For each fruit, we calculated the proportion of viable seeds, assessing viability based on
976 visible malformations. We confirmed inviability by performing germination assays (100
977 seeds plated across 5 replicate plates of 0.6% agar for each cross. Plates were cold
978 stratified for one week, then transferred to warm, long days in the Duke growth

979 chambers. Final germination was recorded after three weeks). Results based on

980 germination assays and morphologically assessed HSI agree qualitatively (r^2= 0.66,

981 df=137, p<0.0001; Supplemental Figure 6 & 7). We therefore focus on morphologically

982 determined HSI (results based on germination proclivity are presented in the

983 supplement). We calculated reproductive isolation (Ramsey & Schemske 2003):

984

985 $$\mathrm{RI} = \frac{\text{Average hybrid seed viability in interspecific crosses}}{\text{Average seed viability in intraspecific crosses}}$$

986

987 and the symmetry of reproductive isolation:

988

989 $$\text{symmetry of RI} = \frac{(\text{proportion viable seeds, DxG}) - (\text{proportion viable seeds, GxD})}{(\text{proportion viable seeds, DxG}) + (\text{proportion viable seeds, GxD})}$$

990

991 Where 'G' and 'D' refer to *Mimulus guttatus* and *Mimulus decorus,* respectively.

992 These values are bounded between -1 and 1. Values closer to -1 indicate an asymmetry

993 where seeds fail when *M. decorus* is the maternal donor and values closer to 1 indicate an

994 asymmetry where seeds fail when *M. guttatus* is the maternal donor, and values close to

995 0 indicate little asymmetry (but do not denote the severity of HSI).

996

997 **Assessing the role of parental conflict in hybrid seed inviability**

998 Each population of *M. guttatus* exhibited a consistent crossing phenotype when
999 crossed to multiple populations of *M. deorus* (i.e. Supplemental Figure 4), but we found
1000 substantial variation between populations of *M. decorus* in the magnitude and the
1001 direction of HSI (Supplemental Figure 5). While some of the variation in HSI between
1002 populations of *M. decorus* and *M. guttatus* can be attributed to variation in ploidy within
1003 *M. decorus*, we also find that the two genetic clades of *M. decorus* exhibit oppositely
1004 asymmetric HSI with *M. guttatus.* That is to say, HSI manifests when northern *M. decorus*
1005 are the maternal contributors in crosses to *M. guttatus,* while HSI manifests when
1006 southern *M. decorus* are the paternal contributor in crosses to *M. guttatus.*

1007 If HSI is largely driven by parental conflict, we would predict (1) hybrid seeds
1008 should display parent-of-origin effects on growth and development, resulting in a size
1009 difference between reciprocal F1s. Specifically, populations that have stronger conflict
1010 should produce hybrid seeds which are larger when they are the paternal donor and
1011 smaller when they are the maternal donor when crossed to a population with weaker
1012 conflict. (2) The magnitude of asymmetry in growth defects between reciprocal F1s
1013 should correspond to the magnitude of HSI. (3) Inferences of the presumed level of
1014 conflict that each species has experienced (e.g. EBN) should predict of the outcomes of
1015 untested crosses.

1016 **1) Prediction 1: Assessing parent-of-origin effects on resource allocation to**
1017 **offspring**

1018 We measured parent of origin effects on resource allocation to offspring using
1019 two approaches: 1) we used photographs to measure total seed width for all hybrid and
1020 parental crosses in ImageJ (Scheider *et al.* 2012), 2) we sought to assess development of
1021 hybrid and parental seeds using crosses between *M. guttatus* and a focal population
1022 from each of northern and southern *M. decorus*. To do this, we crossed plants, as in
1023 above, but collected fruits at 4,6,8,10 and 14 Days After Pollination (DAP). Fruits were
1024 collected and immediately placed in FAA fixative (10 Ethanol: 1 Glacial acetic acid: 2
1025 Formalin: 7 H_20). Fruits were processed in a similar manner to White & Turner (2012).
1026 In brief, after at least 24 hours in fixative, fruits were gradually dehydrated in a Tert-
1027 Butyl alcohol (TBA) dehydration series, then mounted in paraffin wax with ~5% gum
1028 elemi resin. Paraffin mounted specimens were then sliced to 8 micron ribbons and
1029 mounted onto slides. We performed a staining series using Safranin-O and Fast-Green,
1030 which stain for nucleic acids and carbohydrates, respectively. We visualized and
1031 photographed seeds from a single fruit for each cross type and time point combination.
1032

1033 **2) Prediction 2: Assessing the correlation between the magnitude of**
1034 **asymmetry in growth defects between reciprocal F1s and HSI**

1035 Using the measurements of seed width from above, we simply correlated the
1036 degree of symmetry of HSI and the degree of symmetry in reciprocal F1 seed size to
1037 determine if the magnitude of growth defect differences were related to the extent of
1038 HSI.
1039

1040 **3) Assessing whether our designations of conflict predict HSI in subsequent**

1041 **crosses**

1042 While other studies have used proxies for the extent of differences in

1043 EBN/inferred conflict between species (e.g. mating system or ploidy; e.g. Lafon-Placette

1044 *et al.* 2018), the species we describe here are all highly outcrossing diploids (for example,

1045 they do not differ in anther-stigma separation; Fig. 5), and potential drivers of variation

1046 in the level of conflict that different species experience are unknown. We therefore use

1047 the patterns of HSI, reciprocal F1 seed sizes, and hybrid seed development between *M.*

1048 *guttatus* and each clade of diploid *M. decorus* to infer EBN/the extent of conflict that

1049 different species have experienced. This mirrors earlier work on EBNs, wherein focal

1050 species were crossed to a common test line to infer EBN, then specific predictions were

1051 formed based on the inferred EBNs and tested using subsequent crosses between lines

1052 with inferred EBNs (i.e. Johnson 1980, Lin 1984). In our case, if parental conflict drives

1053 HSI, then we infer that northern *M. decorus* must have weaker conflict than *M. guttatus,*

1054 as hybrid seeds between the two species are larger and display excessive endosperm

1055 development when northern *M. decorus* is the maternal parent, but smaller and exhibit

1056 more precocious endosperm development when northern *M. decorus* is the paternal

1057 parent. In contrast, we infer that southern *M. decorus* has stronger conflict than *M.*

1058 *guttatus,* because when *M. guttatus* and southern *M. decorus* are crossed, seeds display a

1059 paternal-excess phenotype when southern *M. decorus* is the paternal genotype, and a

1060 maternal-excess phenotype when *M. guttatus* is the paternal parent. We can then use

1061 these inferences to make predictions about subsequent, untested crosses, if HSI is driven
1062 by patterns of conflict.

1063 Parental conflict theory predicts that populations that show the most extreme
1064 levels of conflict should display the strongest reproductive isolation, and this
1065 reproductive isolation should be accompanied by differences in reciprocal F1 seed size.
1066 To test this, we performed two additional sets of crosses. Firstly, we leveraged the
1067 diversity of inferred EBNs between diploid species by crossing accessions from all
1068 populations of the northern and southern clades of diploid *M. decorus* to a focal
1069 accession from each clade (*IMP* from the northern clade; *Odell Creek* from the southern
1070 clade). As these clades are presumed to exhibit the most extreme difference in parental
1071 conflict, we would predict that they should exhibit the most extreme HSI, and that
1072 patterns of HSI should be accompanied by differences in reciprocal F1 seed sizes,
1073 wherein F1 seeds are larger when northern *M. decorus* is the maternal parent. Secondly,
1074 we leveraged diversity in inferred EBNs caused by differences in ploidy by crossing the
1075 focal accessions from the northern and southern clades of *M. decorus* from above to all
1076 populations of tetraploid *M. decorus*. If parental conflict is driving patterns of HSI in this
1077 group, we would predict that crosses between tetraploids and low-conflict northern *M.*
1078 *decorus* should exhibit more extreme HSI than crosses between northern *M. decorus* and
1079 *M. guttatus,* and reciprocal F1 seeds should exhibit differences in growth and
1080 development. In contrast, southern *M. decorus* should exhibit much less, if any, HSI
1081 when crossed to tetraploid *M. decorus* as these two clades exhibit a smaller difference in

1082 presumed conflict. Accordingly, reciprocal F1 seeds should exhibit minimal differences
1083 in growth and development. We also crossed all four populations of *M. guttatus* used
1084 above in all possible combinations to determine if alleles that contribute to HSI were
1085 naturally segregating throughout *M. guttatus*. Crosses were processed as above to score
1086 average seed viability based on morphology, average germination rate, and average
1087 size.

1088
1089
1090

1091 QUANTIFICATION AND STATISTICAL ANALYSIS

1092 Phenotypic analyses

1093 To determine how species varied in multivariate trait space, we completed a
1094 PCA of all traits, with traits scaled to have unit variance. PCs 1 and 2 accounted for
1095 47.84% and 19.58% trait variance, respectively, and were the only PCs to explain a
1096 significant amount of variance using a broken stick model.

1097

1098 Genotypic analyses

1099 *Genome Re-sequencing: Processing of Files*

1100 For population genomic analyses, we used only the whole-genome sequences.
1101 For these samples, we trimmed adapter and low-quality sequences using Trim Galore!
1102 (Kreuger 2015), then aligned the trimmed sequences to the *M. guttatus* Version 2.0 hard
1103 masked reference genome using BWA *mem* (Li & Durbin 2009;
1104 https://phytozome.jgi.doe.gov/). We cleaned, sorted and marked duplicate reads using

1105 Picard tools (Li *et al.* 2009), then used *HaplotypeCaller* in GATK to call SNPs for each
1106 genome separately, and finally performed *GenotypeGVCFs* in GATK with all samples
1107 and both variant and invariant sites (McKenna *et al.* 2010). We then filtered the resultant
1108 VCF file to remove INDELs, and keep sites with a minimum quality score of 30 and a
1109 depth of coverage of 5x per individual using VCFtools (Danecek *et al.* 2011).
1110 For PCA analyses we combined the whole genome re-sequence data with
1111 previously published GBS dataset from Twyford & Friedman (2015). For these samples,
1112 we processed the raw reads from Twyford and Friedman (2015) similarly, but split
1113 individuals by barcode, discarded low quality reads, and trimmed barcodes using
1114 STACKs before alignment (Catchen *et al.* 2013).
1115
1116 *Population Genomic Analyses*
1117 To estimate diversity and divergence among taxa, we used only diploid, whole-
1118 genome re-sequenced accessions. We first filtered the VCF file to retain only 4-fold
1119 degenerate sites, remove INDELs and retain sites with a quality score =/>30 and a
1120 minimum read depth of 5x. This left 1,201,466 sites total (including both variant and
1121 invariant sites). We then estimated within-species diversity and between species
1122 divergence and differentiation by calculating pairwise nucleotide diversity (π), d_{xy}, *and* F_{st}
1123 in non-overlapping 500 kb windows using custom Python scripts courtesy of Simon
1124 Martin (available: https://github.com/simonhmartin/genomics_general). Both variant
1125 and invariant sites were used to calculate π and d_{xy}, which were estimated by dividing
1126 the total number of pairwise differences by the total number of genotyped sites for

1127 within and between-species, respectively. Estimates of divergence and differentiation
1128 were completed for each pairwise comparison of the 5 species (20 comparison), while
1129 nucleotide diversity was calculated for each species separately. Genome-wide averages
1130 were then calculated.
1131
1132 *Phylogenetic Analyses*
1133 We next constructed Neighbor-Joining (NJ) trees to infer relationships among
1134 diploid taxa in our sample. We further filtered the VCF to retain only sites with <5%
1135 missing data, leaving 25,765 SNPs for analyses. We then constructed a consensus NJ tree
1136 using the *ape* package in R (Paradis & Schliep 2018). We also calculated 56 NJ trees for
1137 500 SNP windows, with a step size of 100 SNPs to assess the level of discordance
1138 throughout the genome (Fig. S3), and plotted a densitree using the *phangorn* package in
1139 R (Schliep. 2011). All trees were rooted the outgroup *M. dentilobus.*
1140
1141 *Principal Components Analyses*
1142 To summarize genetic relationships among diploid accessions we performed a
1143 PCA using ANGSD (Korneliussen *et al.*2014). ANGSD uses .bam files to calculate a
1144 genotype likelihood at each site, and is therefore able to integrate genotype uncertainty
1145 into various analyses, which is useful for low-coverage re-sequencing or GBS data. For
1146 our PCA analyses, we filtered our dataset to keep sites that contained a minimum
1147 mapping quality score of 30 or above, a base quality score of 20 or above, and contained

1148 genotypic information for at least ~85% of accessions (i.e. 203/238), which leaves a total
1149 of 25,405 sites. We find that PCs 1-6 explained a significant proportion of the variation
1150 using a broken stick model, with PCs 1 and 2 explaining 33.1% and 25.7% of the
1151 variance, respectively. PCs 3, 4, 5 and 6 accounted for 19.0, 16.3, 10.1, and 5.7% of the
1152 variance, respectively (Fig. S1).

1153 For comparison, we also performed an additional PCA that included only
1154 diploid samples, to determine if the addition of tetraploid samples biased our PCA. The
1155 results from the two analyses qualitatively agree, and the relationships among species in
1156 PC space did not change by the addition of tetraploid individuals (Figure 1; Fig. S2).

1157

1158 **Analyses of crossing data**

1159 To determine the extent of HSI, the extent of pollen/pistil interactions, and
1160 reciprocal F1 seed size differences between *M. guttatus* and *M. decorus,* as well as within
1161 *M. decorus,* we performed series of a linear mixed models using the *lme4* and *car*
1162 packages in the statistical interface R (R Core Team 2017; Bates *et al.* 2015; Fox &
1163 Weisberg 2011). To determine the extent of HSI and pollen/pistil interactions, we used
1164 the proportion of viable seeds per fruit and the total number of seeds produced as the
1165 dependent variable, respectively. Cross type, genetic clade, and their interaction were
1166 treated as fixed effect predictor variables, while population was treated as a random
1167 effect, and the maternal and paternal individual used in each cross were treated as
1168 random effects nested within population. We find a significant interaction effect

between cross type and genetic clade for the proportion of viable seeds, and so also performed these linear mix-models on each clade separately, again treating population as a random effect and the maternal and paternal individual used as random effects nested within population. In all cases where cross type was significant, we performed a *post hoc* pairwise T-test with Holm correction for multiple testing to determine which crosses differed significantly.

To determine the extent of size differences between reciprocal F1s, we also performed a linear mixed model on seed widths with cross type as a fixed effect and population as a random effect. As seeds were pooled in order to photograph them, the exact maternal and paternal individual were unknown for each particular seed, and therefore could not be included in the model. These analyses were done for each genetic clade separately.

To assess differences in stigma-anther separation, we first averaged the distance between the stigma and the upper and lower sets of anthers. We then performed a linear mixed model on the average stigma-anther separation with genetic clade as a fixed effect and maternal family as a random effect.

KEY RESOURCES TABLE

Reagent or Resource	Source	Identifier
Chemicals		
FAA	JMC	10 Ethanol: 1 Glacial acetic acid: 2 Formalin: 7 H_20

Cystain UV Precise P buffer	Sysmex	Catalogue number: 05-5002
DAPI (4′,6-diamidino-2-phenylindole)	ThermoFisher Scientific	Catalogue number: D1306
Safranin-O	Sigma-Aldrich	Catalogue number: S2255-25G
Fast-Green	Sigma-Aldrich	Catalogue number: F7252-5G
Critical commercial assays		
Genejet extraction kit	ThermoFisher Scientific	Catalogue number: K0691
Nextra library kit	Illumina	Catalogue number: FC-131-1024
Deposited data		
Re-sequence genomes	This paper; Puzey *et al.* 2017	
Experimental models		
Mimulus	Seeds collected by JMC, or generously given to JMC by former members of the Willis lab	
Software and algorithms		
TrimGalore!	Kreuger 2015	
BWA	Li & Durbin 2009	
GATK	McKenna *et al.* 2010	
VCFTools	Danecek *et al.* 2011	
ANGSD	Korneliussen *et al.*2014	
Genome Tools	Python scripts provided by Simon Martin	https://github.com/simonhmartin/genomics_general
R: *ape*	Paradis & Schliep. 2018	

R: *phangorn*	Schliep. 2011	
R: *lme4*	Bates *et al.* 2015	
R: *car*	Fox & Weisberg 2011	
Stacks	Catchen *et al.* 2013	

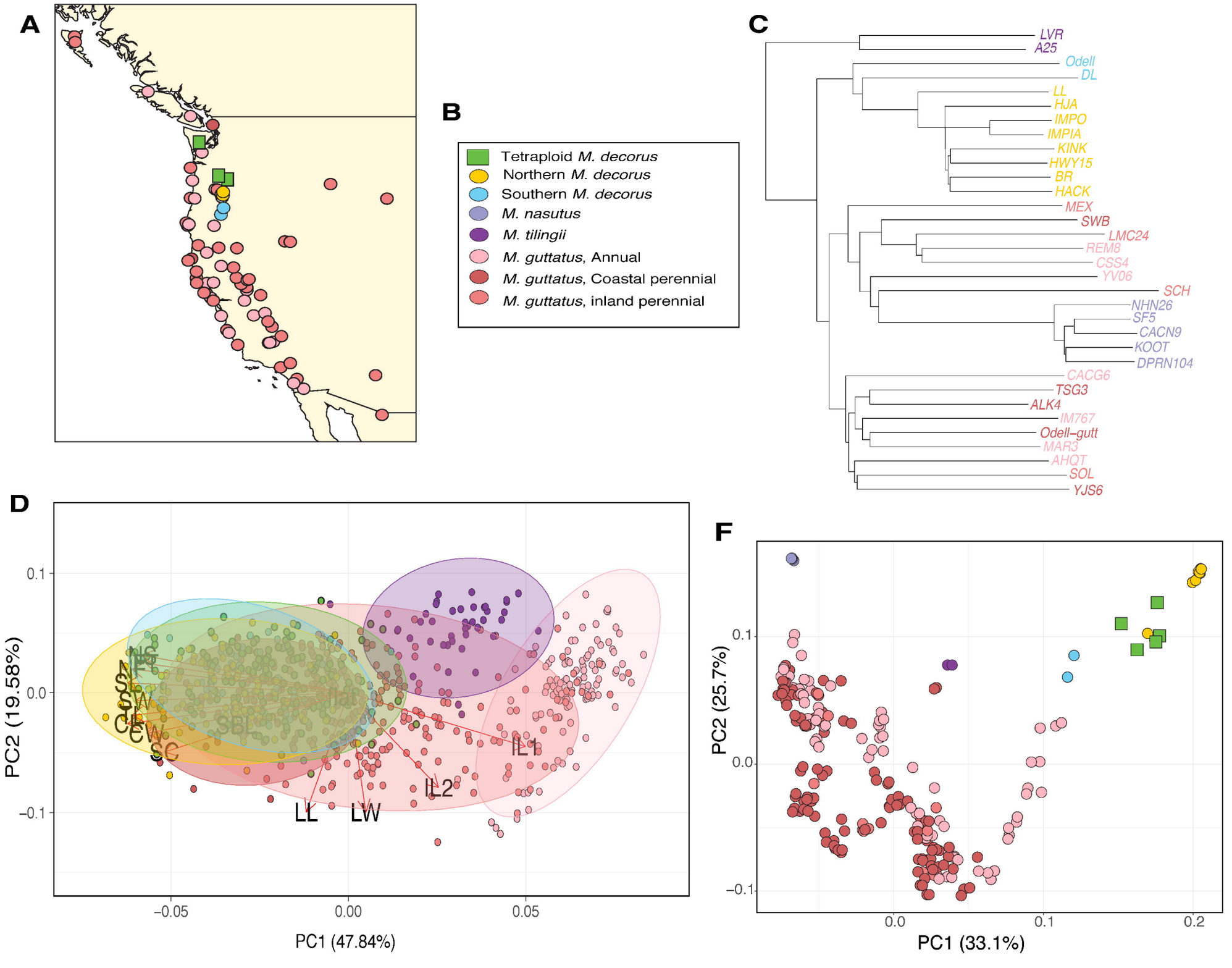
A
B
Tetraploid M. decorus
Northern M. decorus
Southern M. decorus
M. nasutus
M. tilingii
M. guttatus, Annual
M. guttatus, Coastal perennial
M. guttatus, inland perennial
C
LVR
A25
Odell
DL
LL
HJA
IMPO
IMPIA
KINK
HWY15
BR
HACK
MEX
SWB
LMC24
REM8
CSS4
YV06
SCH
NHN26
SF5
CACN9
KOOT
DPRN104
CACG6
TSG3
ALK4
IM767
Odell–gutt
MAR3
AHQT
SOL
YJS6
D
PC2 (19.58%)
PC1 (47.84%)
0.1
0.0
−0.1
−0.05
0.00
0.05
SL
SW
CL
CW
SC
SBL
IL1
IL2
LL
LW
F
PC2 (25.7%)
PC1 (33.1%)
0.1
0.0
−0.1
0.0
0.1
0.2

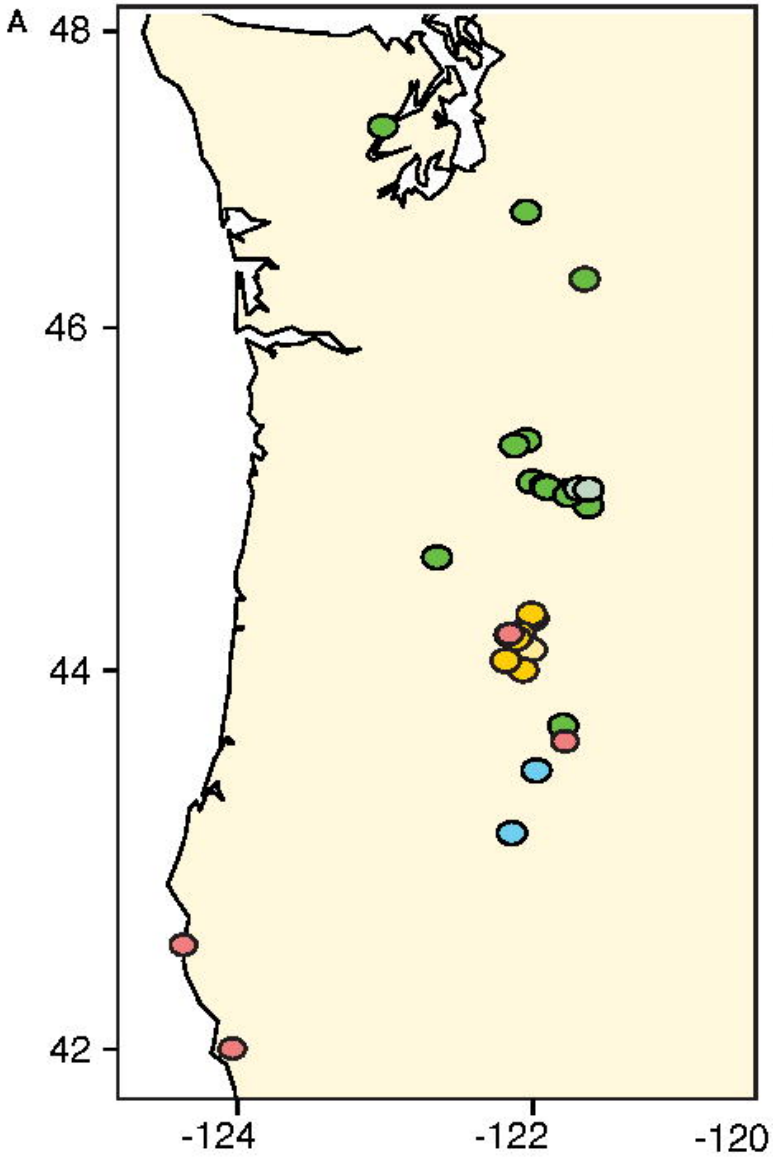
A
48
46
44
42
-124
-122
-120

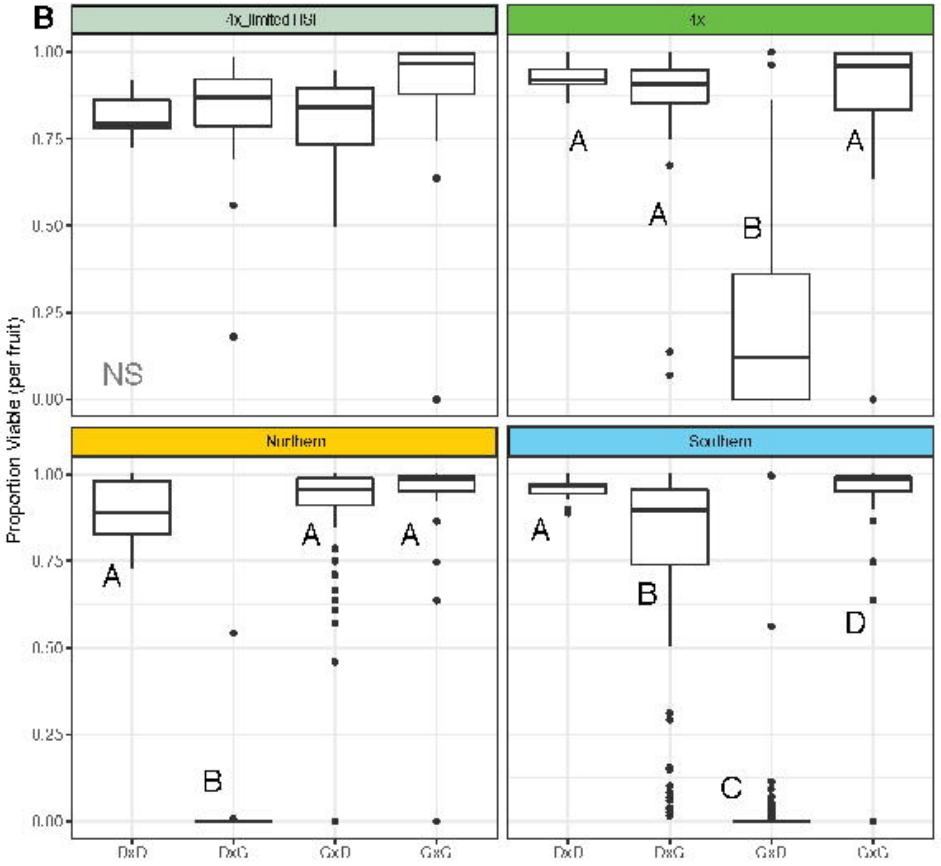
B
4x_limited ISI
4x
Northern
Southern
Proportion Viable (per fruit)
1.00
0.75
0.50
0.25
0.00
NS
A
B
A
A
A
A
B
C
D
DxD
DxG
GxD
GxG

C
D

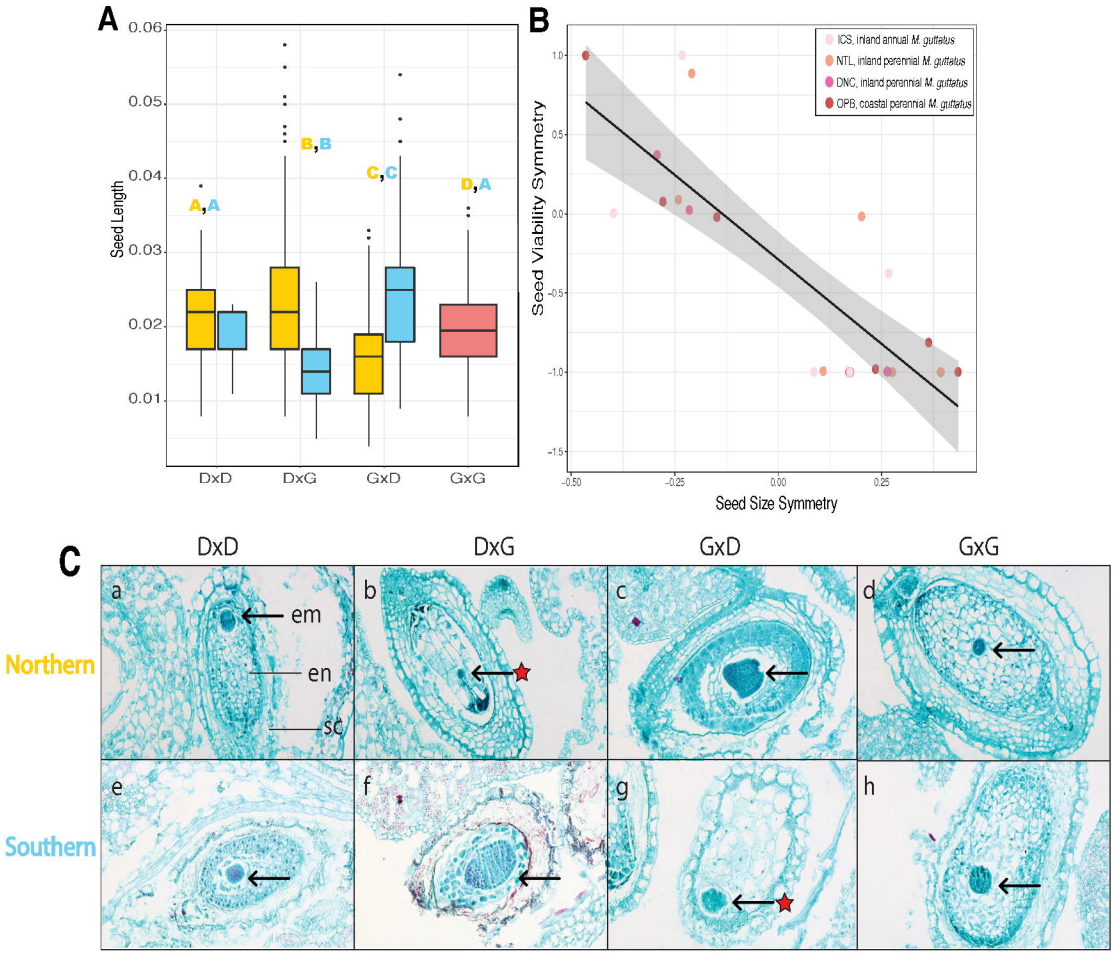
A
Seed Length
0.06
0.05
0.04
0.03
0.02
0.01
A,A
B,B
C,C
D,A
DxD
DxG
GxD
GxG
B
Seed Viability Symmetry
Seed Size Symmetry
ICS, inland annual M. guttatus
NTL, inland perennial M. guttatus
DNC, inland perennial M. guttatus
OPB, coastal perennial M. guttatus
1.0
0.5
0.0
−0.5
−1.0
−1.5
−0.50
−0.25
0.00
0.25
C
DxD
DxG
GxD
GxG
Northern
Southern
a
b
c
d
e
f
g
h
em
en
sc

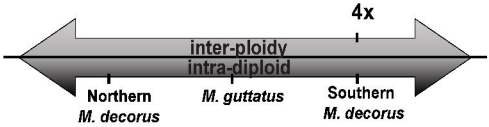
4x
inter-ploidy
intra-diploid
Northern
M. decorus
M. guttatus
Southern
M. decorus

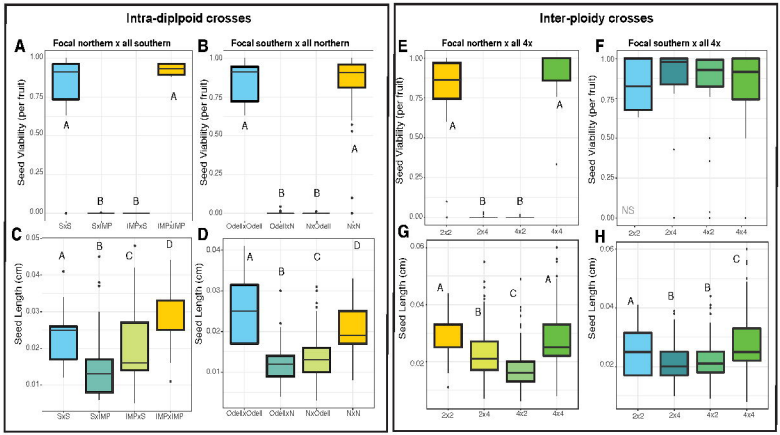
Intra-diplpoid crosses
Inter-ploidy crosses
Focal northern x all southern
Focal southern x all northern
Focal northern x all 4x
Focal southern x all 4x
Seed Viability (per fruit)
Seed Length (cm)
SxS
SxIMP
IMPxS
IMPxIMP
OdellxOdell
OdellxN
NxOdell
NxN
2x2
2x4
4x2
4x4
NS

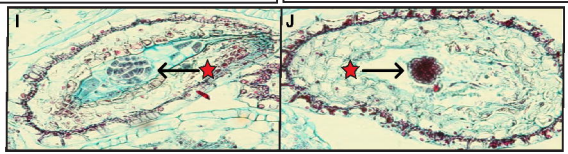
I
J

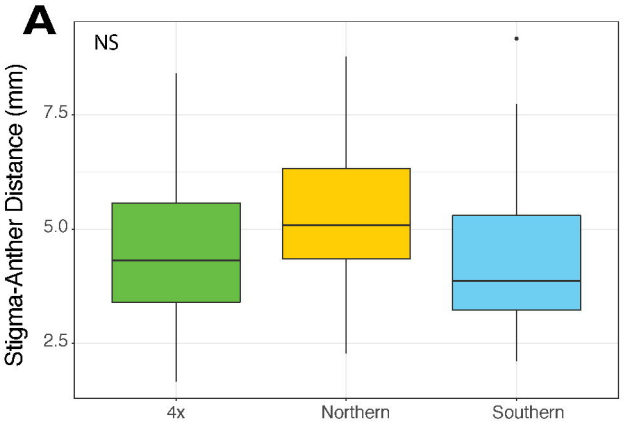
A
NS
Stigma-Anther Distance (mm)
7.5
5.0
2.5
4x
Northern
Southern

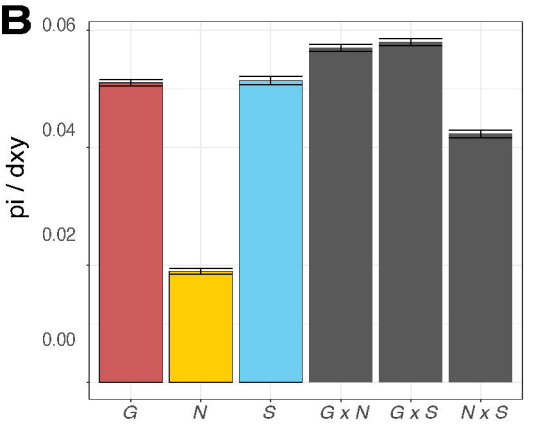
B
pi / dxy
0.06
0.04
0.02
0.00
G
N
S
G x N
G x S
N x S